

000 001 002 003 004 005 006 007 008 009 010 011 012 013 014 015 016 017 018 019 020 021 022 023 024 025 026 027 028 029 030 031 032 033 034 035 036 037 038 039 040 041 042 043 044 045 046 047 048 049 050 051 052 053 TRIVLA: A TRIPLE-SYSTEM-BASED UNIFIED VISION-LANGUAGE-ACTION MODEL WITH EPISODIC WORLD MODELING FOR GENERAL ROBOT CONTROL

Anonymous authors

Paper under double-blind review

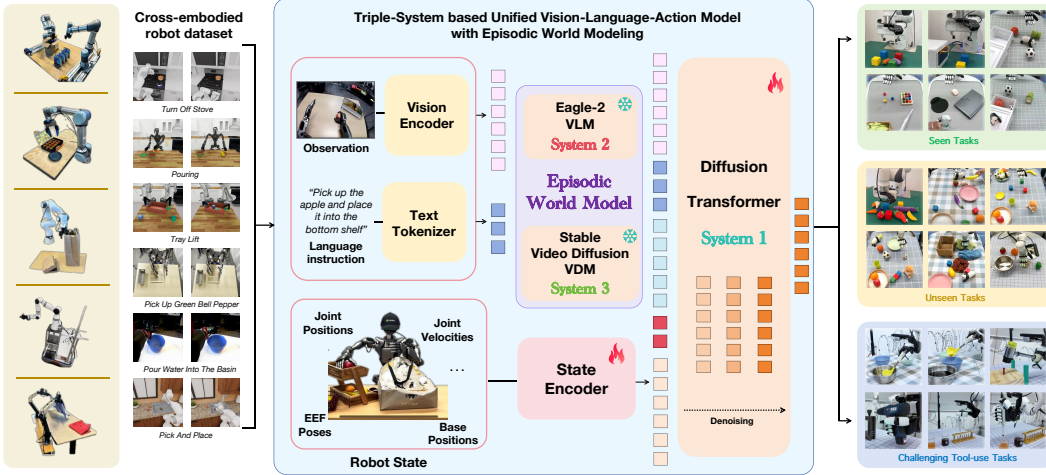


Figure 1: **TriVLA** is a unified Vision-Language-Action framework that adopts a triple-system architecture inspired by the **episodic world model**. Image and language inputs are processed by a Vision-Language Model for multimodal perception. A Video Diffusion Model provides dynamic world modeling and future prediction. The policy module integrates sequential outputs, robot state, and action history and generates real-time actions for complex manipulation tasks.

ABSTRACT

Recent advances in vision–language models (VLMs) have enabled robots to follow open-ended instructions and demonstrate impressive commonsense reasoning. However, current vision–language–action (VLA) frameworks primarily rely on static representations and limited temporal context, restricting agents to short-horizon, reactive behaviors and hindering robust generalization in dynamic embodied environments. Inspired by cognitive neuroscience theories of episodic memory, we are, to our knowledge, among the first to introduce a formalized episodic world model in VLA, enabling embodied robots to accumulate, recall, and predict sequential experiences. As an instantiation of this concept, our unified **TriVLA** realizes the episodic world model through a triple-system architecture: integrating multimodal grounding from a pretrained VLM (System 2) and temporally rich dynamics perception from a video diffusion model (System 3). This enables the agent to accumulate and recall sequential experiences, interpret current contexts, and predict future environmental evolution. Guided by episodic representations that span both the past and anticipated future, the downstream policy (System 1) generates coherent, context-aware action sequences through flow-matching and cross-modal attention mechanisms. Experimental results show that TriVLA operates efficiently at 36 Hz and consistently outperforms baseline models on standard benchmarks and challenging real-world manipulation tasks. It demonstrates strong long-horizon planning and open-ended intent understanding,

[†] Corresponding authors

054 showcasing the advantages of episodic world model-inspired reasoning for robust,
 055 generalizable robot intelligence.
 056

057 1 INTRODUCTION

060 *“Episodic memory is the only memory system that allows mental time travel—backward into the
 061 past and forward into the future.”*

062 — Endel Tulving

064 Building on this cognitive foundation, we advocate that robotic agents, require an internal **episodic**
 065 **world model**: a representational system that not only recalls past interactions but also anticipates
 066 future dynamics, thereby enabling robust generalization in embodied environments.

067 Decades of cognitive neuroscience provide compelling evidence for this perspective. As first ar-
 068 ticulated by Tulving Tulving et al. (1972), episodic memory refers to the encoding, storage, and
 069 retrieval of experiences within their spatiotemporal context. This unique system empowers humans
 070 not only to recollect the past but also to simulate potential futures, thus grounding flexible planning
 071 and adaptive decision-making. Converging findings highlight the central roles of the hippocampus
 072 and prefrontal cortex in supporting episodic memory, enabling individuals to integrate sensory cues
 073 with temporal dynamics to construct predictive internal world models Tulving (2002); Pritzel et al.
 074 (2017); Blundell et al. (2016); Lin et al. (2018); Gershman & Daw (2017). Episodic memory thus
 075 forms a fundamental component of intelligence, providing both the experiential basis for learning
 076 and the representational scaffolding for generalization across novel tasks.

077 Inspired by these insights, we propose the concept of an episodic world model: a unified framework
 078 that integrates multimodal grounding with temporally rich dynamic modeling. Unlike static scene
 079 representations, an episodic world model continuously accumulates, recalls, and predicts sequential
 080 experiences, equipping artificial agents with a memory system more akin to human intelligence.
 081 Recent advances in video diffusion models (VDMs) Blattmann et al. (2023a); Hong et al. (2022);
 082 Yang et al. (2024); Brooks et al. (2024) provide a technological foundation for this paradigm, as
 083 they capture temporal continuity and physical dynamics across video sequences, naturally aligning
 084 with episodic memory principles and enabling richer, context-aware internal representations.

085 In parallel, vision–language models (VLMs) Liu et al. (2024c); Alayrac et al. (2022); Li et al.
 086 (2023a); Zhang et al. (2023); Bai et al. (2023); Gao* et al. (2023); Zhang et al. (2024b;a) have
 087 demonstrated impressive progress in instruction following and commonsense reasoning through
 088 large-scale pretraining on image–text corpora. Extending these capabilities, dual-system archi-
 089 tectures have advanced VLMs into vision–language–action (VLA) models that generate action
 090 plans Ahn et al. (2022); Driess et al. (2023); Huang et al. (2023); Belkhale et al. (2024) and es-
 091 timate SE(3) object poses Brohan et al. (2023); Kim et al. (2024); Li et al. (2024), enabling robots
 092 to map multimodal inputs into generalizable control behaviors. As illustrated in Figure 2, current
 093 VLM-based VLA systems Intelligence et al. (2025); Black et al. (2024); Brohan et al. (2023); Kim
 094 et al. (2024); Pertsch et al. (2025) remain predominantly static: they depend on one or two instant-
 095 aneous observations, overlooking the sequential and dynamic structures that characterize embodied
 096 interaction. As a result, they cannot encode or utilize temporally extended experiences, a capability
 097 similar to human episodic memory and crucial for robust performance in dynamic environments.

098 To bridge this gap, we introduce **TriVLA**, a unified Vision–Language–Action model that imple-
 099 ments the episodic world model through a triple-system compositional architecture. Extending prior
 100 dual-system designs Bjorck et al. (2025); Shi et al. (2025), TriVLA explicitly integrates:

- 100 • System 2: Episodic Multimodal Perception, a pretrained VLM that interprets observations
 101 and instructions, summarizing task goals and contextual cues.
- 102 • System 3: Episodic Dynamics Perception, a video diffusion model fine-tuned on large-
 103 scale human and robotic manipulation datasets Khazatsky et al. (2024); Jin et al. (2024); Lu
 104 et al. (2024), which encodes sequences of past states and predicts future scene trajectories,
 105 realizing episodic context accumulation.

106 Together, Systems 2 and 3 jointly compose the episodic world model, fusing descriptive multimodal
 107 grounding with predictive temporal modeling. This joint representation empowers Policy Learn-

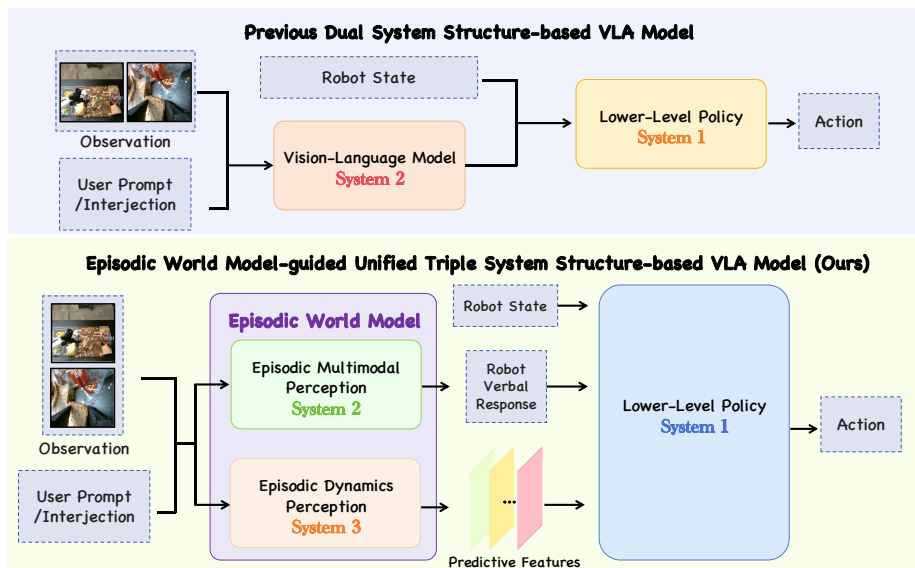


Figure 2: **Comparison between dual-system architectures and our episodic world model-guided TriVLA.** TriVLA implements the **episodic world model** using a triple-system architecture. In contrast, previous dual-system methods relied on static representations and limited temporal context, which restricted agents to short-horizon, reactive behaviors in dynamic environments.

ing (System 1) to flexibly adapt actions based on accumulated experiences and anticipated future dynamics. By continually monitoring motion sequences embedded within the episodic world representation, the downstream policy induces an implicit inverse-dynamics prior Min et al. (2023); Tian et al. (2024). This facilitates the transfer of the generalization capabilities inherent in the episodic world model to the robotic policy, meaning that the robot requires only a limited number of demonstrations to align its action space with the visual domain. During training, System 1 utilizes action flow-matching and cross-attention mechanisms to integrate output tokens from both Systems 2 and 3. It adopts embodiment-specific encoders and decoders to manage variable state and action dimensions during motion generation. In addition, inspired by recent advances in robot learning, System 1 is designed to predict a chunk of actions rather than generating isolated actions at each timestep.

Our main contribution is an episodic world model inspired by cognitive neuroscience theories of episodic memory. Building on this, we introduce a novel triple-system architecture within a unified Vision-Language-Action framework. The episodic world model that guides manipulation policy learning with temporally extended, context-aware signals. As illustrated in Figure 1, this unified framework empowers robots to interpret complex prompts, reason over long horizons, and adapt adaptively in open-ended, dynamic scenarios.

Experimental results demonstrate that the proposed TriVLA consistently outperforms baseline algorithms, in both simulated Mees et al. (2022); Liu et al. (2024a); Yu et al. (2020) and real-world environments. This highlights its effectiveness in aligning with human intent and achieving long-horizon task success. Notably, TriVLA attains improvements of 0.21, 0.11, and 0.13 on the Calvin ABC→D, LIBERO, and MetaWorld benchmarks, respectively, compared to prior state-of-the-art methods. In real-world experiments, TriVLA demonstrates strong effectiveness in dexterous hand manipulation tasks, particularly in long-horizon scenarios.

The contributions of this paper are summarized:

- **Episodic World Model Inspired by Cognitive Neuroscience:** We propose an episodic world model for embodied agents, inspired by cognitive neuroscience theories of episodic memory. This model enables robots to accumulate, recall, and predict sequential multimodal experiences and offers a solid foundation for robust, adaptive control.
- **A Unified Triple-System Compositional Architecture:** Building on this foundation, we present TriVLA, a triple-system architecture implementing the episodic world model.

162 TriVLA provides high-level reasoning and dynamic prediction. Robots using TriVLA can
 163 understand complex prompts and perform long-horizon manipulation.

164

- 165 • **State-of-the-art Performance:** TriVLA outperforms other baseline algorithms, including
 166 novel skill compositions beyond training combinations. This demonstrates the effectiveness
 167 in both alignment with human intent and long-horizon task success.

168

169 2 RELATED WORK

170

171 **Vision-language-action models.** Previous studies Ahn et al. (2022); Driess et al. (2023); Huang
 172 et al. (2023; 2024b) have advanced robotic language-and-vision comprehension to autonomously
 173 generate task plans. Vision-language-action (VLA) models leverage VLM reasoning for $SE(3)$
 174 pose prediction; RT2 Brohan et al. (2023) binarizes 7-DoF actions for autoregressive prediction;
 175 ManipLLM Li et al. (2024) incorporates affordance priors and chain-of-thought reasoning; Open-
 176 VLA Kim et al. (2024) pretrains on Open X-Embodiment O’Neill et al. (2023) for improved general-
 177 alization; and FAST Pertsch et al. (2025) uses discrete cosine transform for scalable prediction. Cog-
 178 nitively inspired dual-systems such as GR00T N1 Bjorck et al. (2025) and Hi Robot Shi et al. (2025)
 179 enhance adaptation to novel scenarios and accelerate task learning. Other VLA approaches Liu et al.
 180 (2024d); Huang et al. (2024a); Li et al. (2023b); Wu et al. (2023) achieve continuous action prediction
 181 by integrating policy heads (MLP, LSTM Graves & Graves (2012)) with regression losses in
 182 imitation learning. Most prior methods are static, relying only on current observations and ignoring
 183 sequential dynamics, limiting their ability to encode temporally extended experiences essential for
 184 robust performance in dynamic environments. In contrast, TriVLA employs a unified triple-system
 185 architecture, enabling robots to interpret complex prompts and perform long-horizon manipulation
 186 tasks across diverse scenarios.

187 **Future prediction in robotics.** Prior studies have explored leveraging future prediction to im-
 188 prove policy learning Bharadhwaj et al. (2024); Chen et al. (2024); Ye et al. (2024); Guo et al.
 189 (2024). SuSIE Black et al. (2023) bases its control policy on a predicted future keyframe from In-
 190 structPix2Pix Brooks et al. (2023), while UniPi Du et al. (2024) models inverse dynamics across
 191 two generated frames. These approaches rely on single-step predictions, which fail to fully cap-
 192 ture complex physical dynamics, and denoising predicted images is time-consuming, reducing con-
 193 trol frequency. GR-1 Wu et al. (2023) generates future frames and actions autoregressively but
 194 produces only one image per forward pass, and its prediction quality lags behind diffusion-based
 195 methods. Seer Tian et al. (2024) predicts actions via inverse dynamics on forecasted visual states,
 196 and VPP Hu et al. (2024) uses video-model representations for generalist robotic policies. In con-
 197 trast, our TriVLA integrates Episodic Multimodal Perception and Episodic Dynamics Perception to
 198 provide both high-level reasoning and dynamic predictive representations, enabling sequential fu-
 199 ture frame prediction while maintaining reasoning to guide policy learning. **Unlike Seer and other**
 200 **single-step predictors, which lack foundation-model priors and cannot support long-horizon rollout,**
 201 **TriVLA uses a fine-tuned video foundation model to generate high-fidelity multi-step predictions**
 202 **for reliable long-horizon reasoning. TriVLA is not merely an incremental extension of VPP or simi-**
 203 **lar methods; it constructs an instruction-conditioned episodic world model that unifies perception,**
 204 **prediction, and decision-making in a single loop.**

205

206 3 PRELIMINARIES

207

208 **Vision-language-action model.** Robotic manipulation remains a core challenge in robotics. Vision-
 209 language-action (VLA) models predict a robot’s next action—typically the end-effector pose—based
 210 on visual observations and human instructions. Recent advances in large pretrained vision-language
 211 models (VLMs) have enabled strong generalization across diverse, language-conditioned manipula-
 212 tion tasks. Most VLM-based VLA approaches adopt a dual-system architecture inspired by human
 213 cognition Kahneman (2011), supporting higher-level reasoning for complex, long-horizon tasks. At
 214 each timestep t , the high-level system receives images \mathbf{o}_t from base and wrist-mounted cameras and
 215 the open-ended instruction \mathbf{v}_t^{in} to generate reasoning tokens. The low-level policy combines these
 tokens with images and robot states to produce an action token sequence $\mathbf{v}_t^{out} \in \mathcal{V}^n$, where each
 token represents a discrete bin of one dimension in the robot action space. The final robot action is
 obtained via a post-processing function f , yielding $\mathbf{a}_t = f(\mathbf{v}_t^{out})$. **VLA performs diverse manipula-**

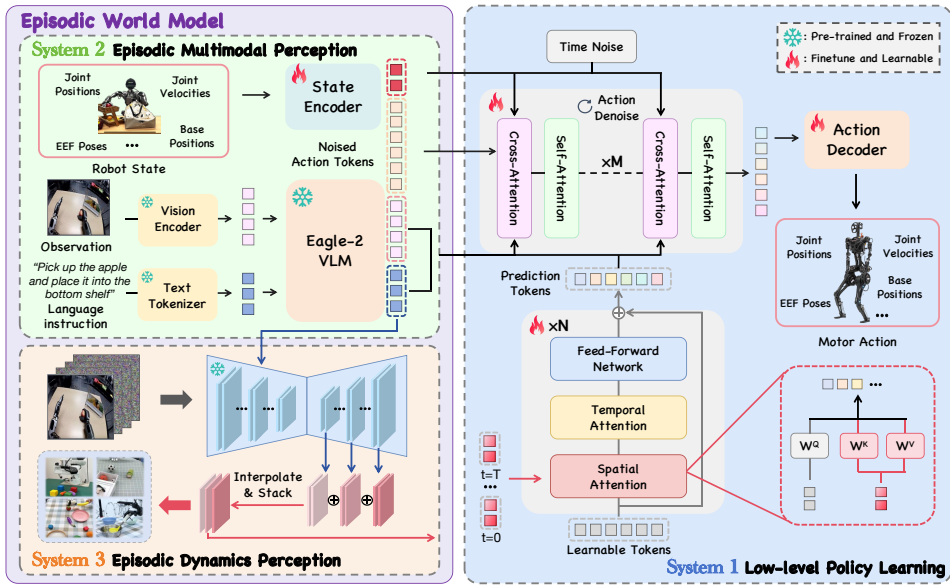


Figure 3: **The pipeline of TriVLA.** TriVLA is a unified Vision-Language-Action framework built on a triple-system paradigm. System 2 employs a pre-trained Eagle-2 VLM for episodic multimodal perception, while System 3 utilizes a general-purpose VDM to model episodic dynamics and sequential changes. Together, these modules form a joint episodic world model with rich, temporally extended representations. System 1 serves as the policy module, applying action flow-matching to integrate all outputs along with robot state and action history.

tion tasks in unstructured, real-world environments by learning generalizable visuomotor behavior from visual observations and language instructions. It is trained via supervised imitation learning on demonstration trajectories.

4 OUR PROPOSED TRIVLA

TriVLA implements the episodic world model using a triple-system design (Figure 3). It integrates (i) Episodic Multimodal Perception, which uses the Eagle-2 VLM Li et al. (2025) to interpret visual inputs and language instructions, and (ii) Episodic Dynamics Perception, where a video diffusion model fine-tuned on large-scale manipulation datasets predicts future scene trajectories. These modules provide rich episodic context for policy generalization.

4.1 EPISODIC MULTIMODAL PERCEPTION (SYSTEM 2)

To realize this component, TriVLA employs the NVIDIA Eagle-2 vision-language model (VLM) Li et al. (2025), pretrained on large-scale internet corpora to jointly interpret observations and instructions, summarizing task goals and contextual cues. Eagle-2 is built from a SmollM2 language model and a SigLIP-2 image encoder, aligned through a broad vision-language pretraining protocol. Images are encoded at a resolution of 224×224 pixels and then processed via pixel shuffle to produce 64 image token embeddings per frame. These image embeddings are jointly encoded with textual input by the LLM component of Eagle-2. The LLM and image encoder are aligned through a general vision-language pretraining protocol covering diverse tasks. During policy training, task descriptions and multiple images are input to the VLM following the chat format established during pretraining. The resulting vision-language tokens, denoted as Q_{vl} (batch size \times sequence length \times hidden dimension), are extracted from the LLM. Empirically, extracting embeddings from the 12th layer of the LLM, rather than from the final layer, yields faster inference and higher policy success rates. To handle varying robot state dimensions, TriVLA uses an embodiment-specific MLP to project each robot’s state into a shared embedding space, resulting in a state token Q_s . **System 2 (Episodic Multimodal Perception)** maintains an online representation of past observations and instructions, capturing relevant context throughout the episode. This representation serves as the model’s episodic memory, enabling informed decision-making based on accumulated history.

270 4.2 EPISODIC DYNAMICS PERCEPTION (SYSTEM 3)
271

272 To infuse extensive prior knowledge of dynamics into policy learning, we fine-tuned the 1.5B-
273 parameter open-source Stable Video Diffusion (SVD) model Blattmann et al. (2023a) as the Episodic
274 Dynamics Perception module for robot manipulation. This video diffusion model, trained on
275 large-scale human and robotic manipulation datasets, encodes sequences of past states and pre-
276 dictes future scene trajectories, enabling episodic context accumulation. By leveraging diverse
277 sources—including internet human manipulation data, robot datasets, and self-collected data—the
278 module robustly models sequential environmental changes essential for effective policy learning.
279 Then Episodic Dynamics Perception module V_θ is trained with diffusion objective, reconstructing
280 the full video sequence $x_0 = s_{0:T}$ in dataset D from noised samples $x_t = \sqrt{\bar{\alpha}_t}x_0 + \sqrt{1 - \bar{\alpha}_t}\epsilon$:

$$281 \mathcal{L}_D = \mathbb{E}_{x_0 \sim D, \epsilon, t} \|V_\theta(x_t, l_{emb}, s_0) - x_0\|^2 \quad (1)$$

282 where l_{emb} denotes the language feature from CLIP Radford et al. (2021). Then we froze the fine-
283 tuned Episodic Dynamics Perception module in downstream action learning.

284 However, denoising a complete video sequence is computationally intensive and may cause open-
285 loop control problems, as highlighted in Du et al. (2024). Furthermore, videos in raw pixel format
286 frequently contain abundant irrelevant information that can hinder effective decision-making. To
287 mitigate these challenges, we utilize the video diffusion model with a single forward pass. Our key
288 insight is that the initial forward step, despite not producing a clear video, offers a coarse trajectory of
289 future states and informative guidance. This observation is validated experimentally and illustrated
290 in Figure 6. Specifically, we concatenate the current image s_0 with the final noised latent $q(x_{t'}|x_0)$
291 (typically white noise) and input this combination into the System 2. The latent features are then
292 directly utilized. Previous work Xiang et al. (2023) emphasizes that up-sampling layers in diffusion
293 models produce more effective feature representations. The feature at the m^{th} up-sampling layer,
294 with width W_m and height H_m , can be expressed as:

$$295 L_m = V_\theta(x_{t'}, l_{emb}, s_0)_{(m)}, L_m \in \mathbb{R}^{T \times C_m \times W_m \times H_m} \quad (2)$$

296 To efficiently integrate features from multiple up-sampling layers while eliminating manual layer
297 selection, we propose an automatic feature aggregation approach across layers. First, each layer’s
298 feature map is linearly interpolated to a common height and width $W_p \times H_p$:

$$299 L'_m = \text{Interpolation}(L_m), L'_m \in \mathbb{R}^{T \times C_m \times W_p \times H_p} \quad (3)$$

300 Subsequently, the features are concatenated along the channel dimension. The final predictive visual
301 representation $F_p \in \mathbb{R}^{T \times (\sum_m C_m) \times W_p \times H_p}$ is given by:

$$302 F_p = \text{concat}((L'_0, L'_1, \dots, L'_m), \text{dim} = 1)$$

303 For robots equipped with multiple camera perspectives, including third-person and wrist-mounted
304 cameras, future states are predicted independently for each view, denoted as $F_p^{static}, F_p^{wrist}$. **System**
305 **3 is not a standalone model. It serves as an *episodic dynamic perception* integrated with Systems 1**
306 **and 2. It processes System 2’s multimodal representations and extracts multi-layer latent dynamics**
307 **via cross-layer aggregation. These features provide episodic context for System 1, enabling accurate**
308 **long-horizon planning. System 3 is the key component that aligns semantics, dynamics, and policy,**
309 **allowing the model to anticipate future outcomes effectively.**

312 4.3 POLICY LEARNING MODULE (SYSTEM 1)
313

314 Systems 2 and 3 together form the episodic world model, combining descriptive multimodal ground-
315 ing with predictive temporal modeling. This combined representation allows System 1 (Policy
316 Learning) to flexibly adapt its actions using both accumulated experience and anticipated future
317 dynamics. The predictive representations generated by the video diffusion model remain high-
318 dimensional because they encode sequences of image features. To efficiently aggregate information
319 across spatial, temporal, and multi-view dimensions, TriVLA compresses these representations into
320 a fixed set of tokens. We initialize learnable tokens $Q_{[0:T,0:L]}$ with fixed length $T \times L$, performing
321 spatial-temporal attention Blattmann et al. (2023b) on each corresponding frame, followed by
322 feed-forward layers. Formally, this branch can be expressed as follows where i is the index of frame:

$$323 Q' = \{\text{Spat-Attn}(Q[i], (F_p^{static}[i], F_p^{wrist}[i]))\}_{i=0}^T \quad (4)$$

$$Q_p = \text{FFN}(\text{Temp-Attn}(Q'))$$

324 **Table 1: Zero-shot long-horizon evaluation on the Calvin ABC→D benchmark (Avg. Len).**

326 Category	327 Method	328 Annotated Data	329 <i>i</i> th Task Success Rate					
			330 1	331 2	332 3	333 4	334 5	335 Avg. Len ↑
330 Direct Action 331 Learning Method	RT-1	100%ABC	0.533	0.222	0.094	0.038	0.013	0.90
	Diffusion Policy	100%ABC	0.402	0.123	0.026	0.008	0.00	0.56
	Robo-Flamingo	100%ABC	0.824	0.619	0.466	0.331	0.235	2.47
332 Future Prediction 333 Related Method	3D Method	100%ABC	0.942	0.842	0.734	0.622	0.507	3.65
	Uni-Pi	100%ABC	0.560	0.160	0.080	0.080	0.040	0.92
	MDT	100%ABC	0.631	0.429	0.247	0.151	0.091	1.55
	Susie	100%ABC	0.870	0.690	0.490	0.380	0.260	2.69
	GR-1	100%ABC	0.854	0.712	0.596	0.497	0.401	3.06
	Vidman	100%ABC	0.915	0.764	0.682	0.592	0.467	3.42
	Seer	100%ABC	0.963	0.916	0.861	0.803	0.740	4.28
	VPP	100%ABC	0.965	0.909	0.866	0.820	0.769	4.33
	TriVLA (ours)	100%ABC	0.968	0.924	0.868	0.832	0.818	4.37
337 Data 338 Efficiency	GR-1	10%ABC	0.672	0.371	0.198	0.108	0.069	1.41
	VPP	10%ABC	0.878	0.746	0.632	0.540	0.453	3.25
	TriVLA (ours)	10%ABC	0.914	0.768	0.644	0.564	0.512	3.46

340 **Table 2: LIBERO benchmark experimental results.**

	Average (↑)	Spatial (↑)	Object (↑)	Goal (↑)	Long (↑)
Diffusion Policy	72.4 ± 0.7%	78.3 ± 1.1%	92.5 ± 0.7%	68.3 ± 1.2%	50.5 ± 1.3%
Octo	75.1 ± 0.6%	78.9 ± 1.0%	85.7 ± 0.9%	84.6 ± 0.9%	51.1 ± 1.3%
OpenVLA	76.5 ± 0.6%	84.7 ± 0.9%	88.4 ± 0.8%	79.2 ± 1.0%	53.7 ± 1.3%
TriVLA (ours)	87.0 ± 0.7 %	91.2 ± 0.8 %	93.8 ± 0.7 %	89.8 ± 0.9 %	73.2 ± 0.5 %

347 After the Episodic Multimodal Perception module (System 2) extracts vision-language tokens Q_{vl} ,
348 and the Episodic Dynamics Perception module (System 3) aggregates future dynamic features into
349 predictive tokens Q_p , a diffusion policy is employed as the action head to generate the action se-
350 quence $a_0 \in A$ conditioned on Q_{vl} and Q_p . The aggregated tokens Q_{vl} and Q_p are integrated into
351 the diffusion transformer blocks via cross-attention layers. The diffusion policy aims to reconstruct
352 the original action a_0 from the noised action $a_k = \sqrt{\beta_k}a_0 + \sqrt{1 - \beta_k}\epsilon$, where ϵ denotes white noise
353 and β_k is the noise coefficient at step k . This process can be interpreted as learning a denoiser D_ψ
354 to approximate the noise ϵ . After the final DiT block, we apply an embodiment-specific action de-
355 coder A_d , implemented as a multi-layer perceptron (MLP). This decoder processes the final tokens
356 to predict actions and minimize the following loss function:

$$\mathcal{L}_{\text{diff}}(\psi; A) = \mathbb{E}_{a_0, \epsilon, k} \|A_d(D_\psi(a_k, Q_{vl}, Q_p)) - a_0\|^2 \quad (5)$$

360 5 EXPERIMENTS

362 **Simulation Benchmarks.** We evaluate our method on three widely used simulation benchmarks
363 for long-horizon manipulation. CALVIN Mees et al. (2022) assesses policies in the challenging
364 ABC→D generalization setting; following GR-1 Wu et al. (2023), we use only language-annotated
365 ABC data for training and testing in the unseen D environment. LIBERO Liu et al. (2024a) consists
366 of four suites (Spatial, Object, Goal, Long), each with 10 tasks and 50 demonstrations. Meta-
367 World Yu et al. (2020); Radosavovic et al. (2023) includes 50 Sawyer-robot tasks.

368 **Real-world Experimental Setups.** We use a KINOVA GEN2 robot with a RealSense D455 depth
369 camera mounted in an eye-to-hand configuration. In an indoor environment, we arranged various ob-
370 jects to encourage generalization of manipulation skills across different scenes. To further evaluate
371 the episodic world model, we designed long-horizon, high-dynamic tasks that require the agent to
372 accumulate, recall, and predict sequential multi-modal experiences. The RealSense D455 captured
373 the entire scene and the robot’s state from both third-person and wrist perspectives.

375 5.1 EXPERIMENTAL RESULTS

377 **Quantitative Results.** Comparisons on the CALVIN benchmark are presented in Table 1. **Zero-shot**
long-horizon evaluation (CALVIN ABC→D) tests the policy on held-out tasks without fine-tuning.

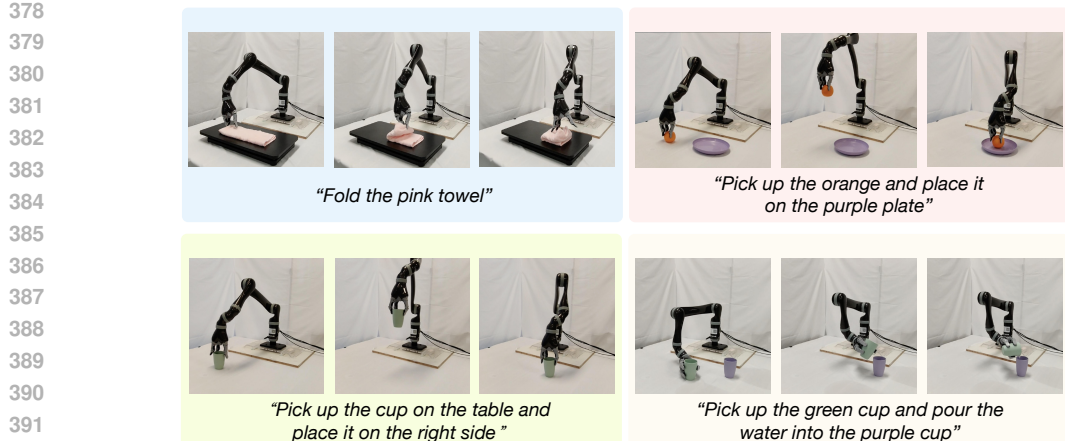


Figure 4: **Qualitative case study of short-horizon tasks.** Our TriVLA performs well on short-horizon tasks. In the real-world tasks, it leverages a triple-system architecture that unifies Episodic Multimodal Perception and Dynamics Perception—both crucial for generalizable policy learning.

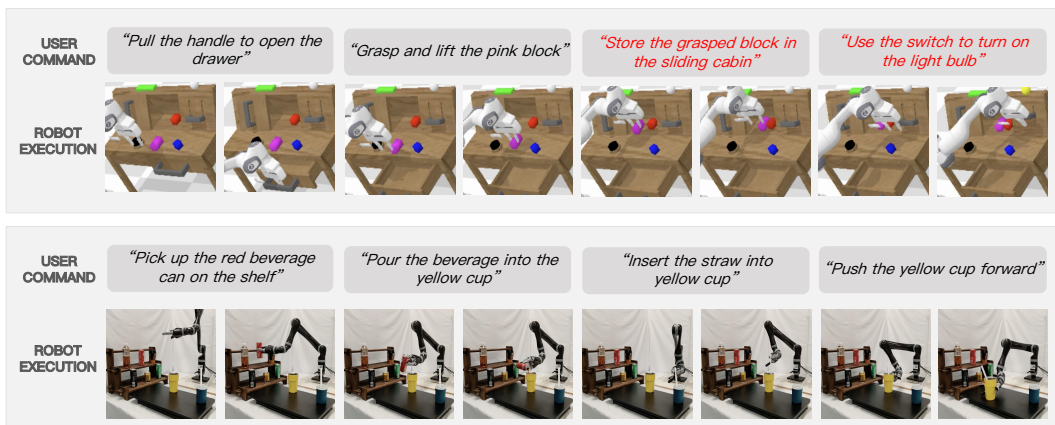


Figure 5: **Qualitative results of long-horizon tasks.** Our TriVLA performs well on long-horizon tasks. In the CALVIN and real-world tasks, it leverages a triple-system architecture that unifies multiple systems for generalizable policy learning.

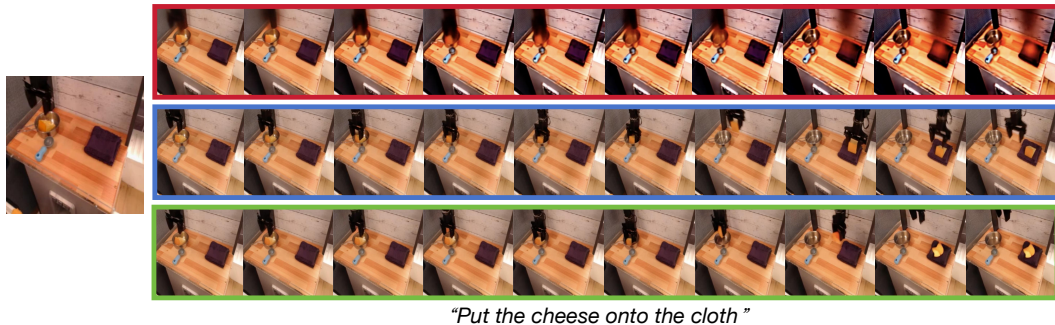
Experimental results for Robo-Flamingo, Susie, GR-1, and 3D Diffuser Actors are taken from their original publications. MDT results come from its official implementation, while RT-1 and UniPi results are from Li et al. (2023b) and Black et al. (2023), respectively. We also evaluated Diffusion Policy using the official open-source code with CLIP-based language conditioning. Our proposed TriVLA significantly outperforms previous state-of-the-art methods. Remarkably, trained on only 10% of the annotated CALVIN ABC dataset, TriVLA achieves an average task completion length of 3.46, surpassing methods trained on the full dataset. It also attains the highest performance on the MetaWorld benchmark (60 tasks; Table 5) and exceeds the strongest VPP baseline in average success rate. Quantitative results on LIBERO are shown in Table 2, with each method evaluated over 500 trials per task suite using 3 random seeds.

The results demonstrate that TriVLA effectively adapts to LIBERO simulation tasks, achieving the best or competitive performance.

Real-World Quantitative Results TriVLA achieves the highest success rates across four real-world tasks (overall 93.5%; Table 3), outperforming Diffusion Policy, Seer, and VPP. While System 2’s multimodal grounding provides modest gains on simple CALVIN tasks, it enables TriVLA to significantly outperform VPP on complex, multi-step instructions like “pre-

Table 5: **Performance on the MetaWorld.**

Method	Easy	Middle	Hard	Avg ↑
RT-1	0.603	0.030	0.014	0.331
Diffusion Policy	0.433	0.072	0.089	0.299
Susie	0.542	0.213	0.244	0.420
GR-1	0.695	0.337	0.448	0.582
VPP	0.822	0.507	0.519	0.679
TriVLA (ours)	0.857	0.528	0.563	0.714



“Put the cheese onto the cloth”

Figure 6: **Visualization of Episodic Dynamics Perception.** The red box indicates one-step prediction, the blue box corresponds to full-step prediction, and the green box marks the ground truth.

Table 3: **Success rates (%) on the Real-World Experiment. We compare our TriVLA with baselines on the real-world experiment. The baselines include Diffusion Policy, Seer, and VPP.**

Method	<i>Fold Towel</i>	<i>Pick up Oranges</i>	<i>Grasp the Cup</i>	<i>Pouring</i>	Overall
Diffusion Policy	34 ± 3	42 ± 4	38 ± 4	32 ± 5	36.5
Seer	66 ± 4	72 ± 6	55 ± 5	66 ± 8	64.8
VPP	85 ± 4	82 ± 8	78 ± 6	72 ± 2	79.3
TriVLA (ours)	96 ± 4	98 ± 2	89 ± 3	91 ± 4	93.5

Table 4: **Success rates (%) on the Real-World Experiment. Sequence of actions: *pick up can* → *pour into cup* → *insert straw* → *push cup*. Baselines include Diffusion Policy, Seer, and VPP.**

Method	<i>Pick up can</i>	<i>Pour into cup</i>	<i>Insert straw</i>	<i>Push cup</i>	Overall
VPP	90 ± 3	73 ± 2	64 ± 6	60 ± 3	71.8
UP-VLA	96 ± 2	92 ± 3	87 ± 1	85 ± 4	90.0
F1	96 ± 3	93 ± 2	89 ± 6	85 ± 3	90.8
TriVLA (ours)	98 ± 2	97 ± 3	94 ± 5	91 ± 2	95.0

pare a drink for a customer” (95.0 vs. 71.8; Table 4) and surpass concurrent VLM–video architectures such as UP-VLA and F1 (95.0 vs. 90.0/90.8), thanks to the integrated design of Systems 1–3 that supports multimodal grounding, episodic recall, and accurate future prediction for long-horizon task execution.

Qualitative Results. Figure 4 and 5 shows two qualitative examples of action sequences in both simulation and the real world. Given multiple consecutive instructions, TriVLA can comprehend intent and leverage prediction to complete long-horizon tasks. These results show that TriVLA supports generalizable policy learning by integrating Episodic Multimodal Perception and Episodic Dynamics Perception. Robots using TriVLA can understand complex sequential prompts, and reason across extended event horizons.

5.2 ABLATION STUDY

Visualization of Episodic Dynamics Perception. We use a stable video diffusion model as the Episodic Dynamics Perception (EDP) module, whose forward pass produces representations capturing both the current scene context and long-horizon future dynamics. Figure 6 visualizes ground-truth futures, single-step predictions, and full-sequence predictions on the Bridge benchmark Walke et al. (2023). While full-sequence predictions remain reasonable, single-step outputs emphasize key motion cues—such as object and robot-arm movements—that support downstream action learning. Overall, the module effectively models entire video sequences and predicts future frames conditioned on current observations and instructions.

Effectiveness of the Episodic Multimodal Perception Module. The System 2 Episodic Multimodal Perception module (EMP), a pretrained Vision-Language Model (VLM), processes visual observations and language instructions to infer task goals. As shown in Table 6 integrating EMP improves performance from 4.06 to 4.37, with inference time increasing from 136 ms to 155 ms, indicating that System 2 substantially enhances action generation accuracy. Similarly, on LIBERO, the inclusion of EMP increases the average success rate from 0.800 to 0.870 (Table 7), demonstrating

486 Table 6: **Sub-system ablation studies on the CALVIN.**
487

488	EMP	EDP	L-Policy	Task Success Rate ↑					Avg.Len ↑	Latency ↓	Params ↓
				1	2	3	4	5			
490	✓	✓	✓	0.914	0.772	0.703	0.622	0.511	3.68	29.29ms	0.53B
491		✓	✓	0.942	0.902	0.843	0.781	0.713	4.04	59.42ms	2.07B
492	✓	✓	✓	0.928	0.896	0.855	0.792	0.705	4.06	115.19ms	1.87B
	✓	✓	✓	0.968	0.924	0.868	0.832	0.818	4.37	142.69ms	3.39B

493 Table 7: **Sub-system ablation studies on the LIBERO.**
494

495	EMP	EDP	L-Policy	Task Success Rate ↑				Avg.SR ↑	Latency ↓	Params ↓
				1	2	3	4			
497		✓	✓	0.728	0.793	0.744	0.529	0.698	30.12ms	0.53B
498	✓	✓	✓	0.813	0.852	0.883	0.682	0.808	58.44ms	2.07B
499	✓	✓	✓	0.822	0.846	0.865	0.668	0.800	118.27ms	1.87B
500	✓	✓	✓	0.912	0.938	0.898	0.732	0.870	141.58ms	3.39B

501 Table 8: **Ablation of Stable Video Diffusion (SVD) in System 3.**
502

	1 (↑)	2 (↑)	3 (↑)	4 (↑)	5 (↑)	Avg.Length(↑)
504	TriVLA (pretrained SVD)	0.931	0.884	0.845	0.776	0.702
505	TriVLA (finetuned SVD)	0.968	0.924	0.868	0.832	0.818

506 Table 9: **Ablation of Predicted Step in System 3.**
507

	1 (↑)	2 (↑)	3 (↑)	4 (↑)	5 (↑)	Avg.Length(↑)
509	TriVLA (1-step)	0.930	0.866	0.842	0.744	0.708
510	TriVLA (2-step)	0.935	0.877	0.841	0.782	0.737
511	TriVLA (4-step)	0.943	0.881	0.840	0.784	0.758
512	TriVLA (8-step)	0.944	0.892	0.854	0.792	0.774
513	TriVLA (16-step)	0.968	0.924	0.868	0.832	0.818
	TriVLA (32-step)	0.962	0.918	0.872	0.844	0.820

514 that System 2 consistently provides significant gains. In the “L-Policy + EDP” ablation, System 2
515 (EMP) is removed, so instructions are fed directly into EDP via CLIP. Without EMP’s multimodal
516 perception, instruction grounding is weaker, limiting performance on complex tasks.
517

518 **Effectiveness of the Episodic Dynamics Perception Module.** The System 3 Episodic Dynamics
519 Perception module (EDP) is a video diffusion model fine-tuned on diverse human and robot manip-
520 ulation datasets to enhance predictive modeling. We ablate System 3 (EDP) by comparing TriVLA
521 variants on CALVIN and LIBERO. On CALVIN, adding EDP to EMP + L-Policy increases average
522 trajectory length from 4.04 to 4.37 across all five tasks (Table 6). On LIBERO, incorporating EDP
523 improves average success rate from 0.808 to 0.870 (Table 7), demonstrating consistent gains and
524 confirming that the full Triple-System (VLM + EDP + Policy) outperforms the Dual-System (VLM
525 + Policy) in long-horizon, dynamic manipulation tasks. Further ablations show that fine-tuning the
526 Stable Video Diffusion (SVD) model is essential: TriVLA with finetuned SVD outperforms pre-
527 trained SVD across all five CALVIN tasks (Avg. Length 4.37 vs. 3.96; Table 8). Horizon ablation
528 also confirms that longer multi-step rollouts consistently improve performance (Avg. Len 3.94 →
529 4.37), highlighting that effective long-horizon manipulation requires true multi-step dynamics mod-
eling rather than trivial single-step extension.
530

531 6 CONCLUSION 532

533 TriVLA is the first framework to formalize an episodic world model within a unified triple-system
534 architecture, drawing inspiration from cognitive neuroscience theories of episodic memory. By in-
535 tegrating multimodal grounding and rich temporal dynamics, TriVLA provides high-level reasoning
536 and dynamic prediction, enabling robots to accumulate, recall, and predict sequential experiences.
537 Experiments show that TriVLA operates efficiently and consistently outperforms state-of-the-art
538 policy baselines. TriVLA significantly improves long-horizon reasoning, sample efficiency, and
539 open-ended goal achievement. These results highlight the potential of episodic world model reason-
ing as a solid foundation for robust and generalizable robot control systems.
540

540 REFERENCES

541

542 Michael Ahn, Anthony Brohan, Noah Brown, Yevgen Chebotar, Omar Cortes, Byron David, Chelsea
543 Finn, Chuyuan Fu, Keerthana Gopalakrishnan, Karol Hausman, et al. Do as i can, not as i say:
544 Grounding language in robotic affordances. *arXiv preprint arXiv:2204.01691*, 2022.

545 Jean-Baptiste Alayrac, Jeff Donahue, Pauline Luc, Antoine Miech, Iain Barr, Yana Hasson, Karel
546 Lenc, Arthur Mensch, Katherine Millican, Malcolm Reynolds, et al. Flamingo: a visual language
547 model for few-shot learning. *Advances in Neural Information Processing Systems*, 35:23716–
548 23736, 2022.

549 Jinze Bai, Shuai Bai, Shusheng Yang, Shijie Wang, Sinan Tan, Peng Wang, Junyang Lin, Chang
550 Zhou, and Jingren Zhou. Qwen-vl: A frontier large vision-language model with versatile abilities.
551 *arXiv preprint arXiv:2308.12966*, 2023.

552

553 Suneel Belkhale, Tianli Ding, Ted Xiao, Pierre Sermanet, Quon Vuong, Jonathan Tompson, Yevgen
554 Chebotar, Debidatta Dwibedi, and Dorsa Sadigh. Rt-h: Action hierarchies using language. *arXiv
555 preprint arXiv:2403.01823*, 2024.

556 Homanga Bharadhwaj, Debidatta Dwibedi, Abhinav Gupta, Shubham Tulsiani, Carl Doersch, Ted
557 Xiao, Dhruv Shah, Fei Xia, Dorsa Sadigh, and Sean Kirmani. Gen2act: Human video generation
558 in novel scenarios enables generalizable robot manipulation. *arXiv preprint arXiv:2409.16283*,
559 2024.

560

561 Johan Bjorck, Fernando Castañeda, Nikita Cherniadev, Xingye Da, Runyu Ding, Linxi Fan,
562 Yu Fang, Dieter Fox, Fengyuan Hu, Spencer Huang, et al. Gr00t n1: An open foundation model
563 for generalist humanoid robots. *arXiv preprint arXiv:2503.14734*, 2025.

564 Kevin Black, Mitsuhiro Nakamoto, Pranav Atreya, Homer Walke, Chelsea Finn, Aviral Kumar, and
565 Sergey Levine. Zero-shot robotic manipulation with pretrained image-editing diffusion models.
566 *arXiv preprint arXiv:2310.10639*, 2023.

567

568 Kevin Black, Noah Brown, Danny Driess, Adnan Esmail, Michael Equi, Chelsea Finn, Niccolo
569 Fusai, Lachy Groom, Karol Hausman, Brian Ichter, Szymon Jakubczak, Tim Jones, Liyiming Ke,
570 Sergey Levine, Adrian Li-Bell, Mohith Mothukuri, Suraj Nair, Karl Pertsch, Lucy Xiaoyang Shi,
571 James Tanner, Quan Vuong, Anna Walling, Haohuan Wang, and Ury Zhilinsky. π_0 : A vision-
572 language-action flow model for general robot control, 2024. URL <https://arxiv.org/abs/2410.24164>.

573

574 Andreas Blattmann, Tim Dockhorn, Sumith Kulal, Daniel Mendelevitch, Maciej Kilian, Dominik
575 Lorenz, Yam Levi, Zion English, Vikram Voleti, Adam Letts, et al. Stable video diffusion: Scaling
576 latent video diffusion models to large datasets. *arXiv preprint arXiv:2311.15127*, 2023a.

577

578 Andreas Blattmann, Robin Rombach, Huan Ling, Tim Dockhorn, Seung Wook Kim, Sanja Fidler,
579 and Karsten Kreis. Align your latents: High-resolution video synthesis with latent diffusion
580 models. In *Proceedings of the IEEE/CVF Conference on Computer Vision and Pattern Recognition*,
581 pp. 22563–22575, 2023b.

582

583 Charles Blundell, Benigno Uria, Alexander Pritzel, Yazhe Li, Avraham Ruderman, Joel Z Leibo,
584 Jack Rae, Daan Wierstra, and Demis Hassabis. Model-free episodic control. *arXiv preprint
585 arXiv:1606.04460*, 2016.

586

587 Anthony Brohan, Noah Brown, Justice Carbajal, Yevgen Chebotar, Joseph Dabis, Chelsea Finn,
588 Keerthana Gopalakrishnan, Karol Hausman, Alex Herzog, Jasmine Hsu, et al. Rt-1: Robotics
589 transformer for real-world control at scale. *arXiv preprint arXiv:2212.06817*, 2022.

590

591 Anthony Brohan, Noah Brown, Justice Carbajal, Yevgen Chebotar, Xi Chen, Krzysztof Choromanski,
592 Tianli Ding, Danny Driess, Avinava Dubey, Chelsea Finn, et al. Rt-2: Vision-language-action
593 models transfer web knowledge to robotic control. *arXiv preprint arXiv:2307.15818*, 2023.

594

595 Tim Brooks, Aleksander Holynski, and Alexei A Efros. Instructpix2pix: Learning to follow image
596 editing instructions. In *Proceedings of the IEEE/CVF Conference on Computer Vision and Pattern
597 Recognition*, pp. 18392–18402, 2023.

594 Tim Brooks, Bill Peebles, Connor Holmes, Will DePue, Yufei Guo, Li Jing, David Schnurr, Joe
 595 Taylor, Troy Luhman, Eric Luhman, Clarence Ng, Ricky Wang, and Aditya Ramesh. Video
 596 generation models as world simulators. 2024. URL [https://openai.com/research/
 597 video-generation-models-as-world-simulators](https://openai.com/research/video-generation-models-as-world-simulators).

598 Xiaoyu Chen, Junliang Guo, Tianyu He, Chuheng Zhang, Pushi Zhang, Derek Cathera Yang,
 599 Li Zhao, and Jiang Bian. Igor: Image-goal representations are the atomic control units for foun-
 600 dation models in embodied ai. *arXiv preprint arXiv:2411.00785*, 2024.

602 Cheng Chi, Zhenjia Xu, Siyuan Feng, Eric Cousineau, Yilun Du, Benjamin Burchfiel, Russ Tedrake,
 603 and Shuran Song. Diffusion policy: Visuomotor policy learning via action diffusion. *The Inter-
 604 national Journal of Robotics Research*, pp. 02783649241273668, 2023.

605 Danny Driess, Fei Xia, Mehdi SM Sajjadi, Corey Lynch, Aakanksha Chowdhery, Brian Ichter,
 606 Ayzaan Wahid, Jonathan Tompson, Quan Vuong, Tianhe Yu, et al. Palm-e: An embodied multi-
 607 modal language model. *arXiv preprint arXiv:2303.03378*, 2023.

609 Yilun Du, Sherry Yang, Bo Dai, Hanjun Dai, Ofir Nachum, Josh Tenenbaum, Dale Schuurmans, and
 610 Pieter Abbeel. Learning universal policies via text-guided video generation. *Advances in Neural
 611 Information Processing Systems*, 36, 2024.

612 Peng Gao*, Jiaming Han*, Renrui Zhang*, Ziyi Lin, Shijie Geng, Aojun Zhou, Wei Zhang, Pan Lu,
 613 Conghui He, Xiangyu Yue, et al. Llama-adapter v2: Parameter-efficient visual instruction model.
 614 *arXiv preprint arXiv:2304.15010*, 2023.

616 Samuel J Gershman and Nathaniel D Daw. Reinforcement learning and episodic memory in humans
 617 and animals: an integrative framework. *Annual review of psychology*, 68(1):101–128, 2017.

618 Raghav Goyal, Samira Ebrahimi Kahou, Vincent Michalski, Joanna Materzynska, Susanne West-
 619 phal, Heuna Kim, Valentin Haenel, Ingo Fruend, Peter Yianilos, Moritz Mueller-Freitag, et al.
 620 The “something something” video database for learning and evaluating visual common sense. In
 621 *Proceedings of the IEEE international conference on computer vision*, pp. 5842–5850, 2017.

623 Alex Graves and Alex Graves. Long short-term memory. *Supervised sequence labelling with recur-
 624 rent neural networks*, pp. 37–45, 2012.

625 Yanjiang Guo, Yucheng Hu, Jianke Zhang, Yen-Jen Wang, Xiaoyu Chen, Chaochao Lu, and Jianyu
 626 Chen. Prediction with action: Visual policy learning via joint denoising process. In *The Thirty-
 627 eighth Annual Conference on Neural Information Processing Systems*, 2024.

629 Wenyi Hong, Ming Ding, Wendi Zheng, Xinghan Liu, and Jie Tang. Cogvideo: Large-scale pre-
 630 training for text-to-video generation via transformers. *arXiv preprint arXiv:2205.15868*, 2022.

632 Yucheng Hu, Yanjiang Guo, Pengchao Wang, Xiaoyu Chen, Yen-Jen Wang, Jianke Zhang, Koushil
 633 Sreenath, Chaochao Lu, and Jianyu Chen. Video prediction policy: A generalist robot policy with
 634 predictive visual representations. *arXiv preprint arXiv:2412.14803*, 2024.

636 Siyuan Huang, Iaroslav Ponomarenko, Zhengkai Jiang, Xiaoqi Li, Xiaobin Hu, Peng Gao, Hong-
 637 sheng Li, and Hao Dong. Manipvqa: Injecting robotic affordance and physically grounded infor-
 638 mation into multi-modal large language models. *arXiv preprint arXiv:2403.11289*, 2024a.

640 Wenlong Huang, Chen Wang, Ruohan Zhang, Yunzhu Li, Jiajun Wu, and Li Fei-Fei. Voxposer:
 641 Composable 3d value maps for robotic manipulation with language models. *arXiv preprint
 642 arXiv:2307.05973*, 2023.

643 Wenlong Huang, Chen Wang, Yunzhu Li, Ruohan Zhang, and Li Fei-Fei. Rekep: Spatio-
 644 temporal reasoning of relational keypoint constraints for robotic manipulation. *arXiv preprint
 645 arXiv:2409.01652*, 2024b.

646 Physical Intelligence, Kevin Black, Noah Brown, James Darpinian, Karan Dhabalia, Danny Driess,
 647 Adnan Esmail, Michael Equi, Chelsea Finn, Niccolò Fusai, Manuel Y. Galliker, Dibya Ghosh,
 648 Lachy Groom, Karol Hausman, Brian Ichter, Szymon Jakubczak, Tim Jones, Liyiming Ke, Devin
 649 LeBlanc, Sergey Levine, Adrian Li-Bell, Mohith Mothukuri, Suraj Nair, Karl Pertsch, Allen Z.

648 Ren, Lucy Xiaoyang Shi, Laura Smith, Jost Tobias Springenberg, Kyle Stachowicz, James Tanner,
 649 Quan Vuong, Homer Walke, Anna Walling, Haohuan Wang, Lili Yu, and Ury Zhilinsky. $\pi_{0.5}$: a
 650 vision-language-action model with open-world generalization, 2025. URL <https://arxiv.org/abs/2504.16054>.

652 Yixiang Jin, Dingzhe Li, Jun Shi, Peng Hao, Fuchun Sun, Jianwei Zhang, Bin Fang, et al. Robotgpt:
 653 Robot manipulation learning from chatgpt. *IEEE Robotics and Automation Letters*, 9(3):2543–
 654 2550, 2024.

655 Daniel Kahneman. *Thinking, fast and slow*. macmillan, 2011.

656 Alexander Khazatsky, Karl Pertsch, Suraj Nair, Ashwin Balakrishna, Sudeep Dasari, Siddharth
 657 Karamchetti, Soroush Nasiriany, Mohan Kumar Srirama, Lawrence Yunliang Chen, Kirsty Ellis,
 658 Peter David Fagan, Joey Hejna, Masha Itkina, Marion Lepert, Yecheng Jason Ma, Patrick Tree
 659 Miller, Jimmy Wu, Suneel Belkhale, Shivin Dass, Huy Ha, Arhan Jain, Abraham Lee, Young-
 660 woon Lee, Marius Memmel, Sungjae Park, Ilija Radosavovic, Kaiyuan Wang, Albert Zhan, Kevin
 661 Black, Cheng Chi, Kyle Beltran Hatch, Shan Lin, Jingpei Lu, Jean Mercat, Abdul Rehman, Pan-
 662 ntag R Sanketi, Archit Sharma, Cody Simpson, Quan Vuong, Homer Rich Walke, Blake Wulfe,
 663 Ted Xiao, Jonathan Heewon Yang, Arefeh Yavary, Tony Z. Zhao, Christopher Agia, Rohan Bai-
 664 jal, Mateo Guaman Castro, Daphne Chen, Qiuyu Chen, Trinity Chung, Jaimyn Drake, Ethan Paul
 665 Foster, Jensen Gao, David Antonio Herrera, Minho Heo, Kyle Hsu, Jiaheng Hu, Donovon Jack-
 666 son, Charlotte Le, Yunshuang Li, Kevin Lin, Roy Lin, Zehan Ma, Abhiram Maddukuri, Suvir Mir-
 667 chandani, Daniel Morton, Tony Nguyen, Abigail O’Neill, Rosario Scalise, Derick Seale, Victor
 668 Son, Stephen Tian, Emi Tran, Andrew E. Wang, Yilin Wu, Annie Xie, Jingyun Yang, Patrick Yin,
 669 Yunchu Zhang, Osbert Bastani, Glen Berseth, Jeannette Bohg, Ken Goldberg, Abhinav Gupta,
 670 Abhishek Gupta, Dinesh Jayaraman, Joseph J Lim, Jitendra Malik, Roberto Martín-Martín, Sub-
 671 ramanian Ramamoorthy, Dorsa Sadigh, Shuran Song, Jiajun Wu, Michael C. Yip, Yuke Zhu,
 672 Thomas Kollar, Sergey Levine, and Chelsea Finn. Droid: A large-scale in-the-wild robot manip-
 673 ulation dataset. 2024.

674 Moo Jin Kim, Karl Pertsch, Siddharth Karamchetti, Ted Xiao, Ashwin Balakrishna, Suraj Nair,
 675 Rafael Rafailov, Ethan Foster, Grace Lam, Pannag Sanketi, et al. Openvla: An open-source
 676 vision-language-action model. *arXiv preprint arXiv:2406.09246*, 2024.

677 Junnan Li, Dongxu Li, Silvio Savarese, and Steven Hoi. Blip-2: Bootstrapping language-image
 678 pre-training with frozen image encoders and large language models. In *International conference
 679 on machine learning*, pp. 19730–19742. PMLR, 2023a.

680 Xiaoqi Li, Mingxu Zhang, Yiran Geng, Haoran Geng, Yuxing Long, Yan Shen, Renrui Zhang,
 681 Jiaming Liu, and Hao Dong. Manipllm: Embodied multimodal large language model for object-
 682 centric robotic manipulation. In *Proceedings of the IEEE/CVF Conference on Computer Vision
 683 and Pattern Recognition*, pp. 18061–18070, 2024.

684 Xinghang Li, Minghuan Liu, Hanbo Zhang, Cunjun Yu, Jie Xu, Hongtao Wu, Chilam Cheang,
 685 Ya Jing, Weinan Zhang, Huaping Liu, et al. Vision-language foundation models as effective robot
 686 imitators. *arXiv preprint arXiv:2311.01378*, 2023b.

687 Zhiqi Li, Guo Chen, Shilong Liu, Shihao Wang, Vibashan VS, Yishen Ji, Shiyi Lan, Hao Zhang,
 688 Yilin Zhao, Subhashree Radhakrishnan, et al. Eagle 2: Building post-training data strategies from
 689 scratch for frontier vision-language models. *arXiv preprint arXiv:2501.14818*, 2025.

690 Zichuan Lin, Tianqi Zhao, Guangwen Yang, and Lintao Zhang. Episodic memory deep q-networks.
 691 *arXiv preprint arXiv:1805.07603*, 2018.

692 Bo Liu, Yifeng Zhu, Chongkai Gao, Yihao Feng, Qiang Liu, Yuke Zhu, and Peter Stone. Libero:
 693 Benchmarking knowledge transfer for lifelong robot learning. *Advances in Neural Information
 694 Processing Systems*, 36, 2024a.

695 Fanfan Liu, Feng Yan, Liming Zheng, Chengjian Feng, Yiyang Huang, and Lin Ma. Robouniview:
 696 Visual-language model with unified view representation for robotic manipulation. *arXiv preprint
 697 arXiv:2406.18977*, 2024b.

702 Haotian Liu, Chunyuan Li, Qingyang Wu, and Yong Jae Lee. Visual instruction tuning. *Advances*
 703 *in neural information processing systems*, 36, 2024c.
 704

705 Jiaming Liu, Mengzhen Liu, Zhenyu Wang, Lily Lee, Kaichen Zhou, Pengju An, Senqiao Yang,
 706 Renrui Zhang, Yandong Guo, and Shanghang Zhang. Robomamba: Multimodal state space model
 707 for efficient robot reasoning and manipulation. *arXiv preprint arXiv:2406.04339*, 2024d.

708 Guanxing Lu, Shiyi Zhang, Ziwei Wang, Changliu Liu, Jiwen Lu, and Yansong Tang. Manigaussian:
 709 Dynamic gaussian splatting for multi-task robotic manipulation. In *European Conference on*
 710 *Computer Vision*, pp. 349–366. Springer, 2024.

711

712 Oier Mees, Lukas Hermann, Erick Rosete-Beas, and Wolfram Burgard. Calvin: A benchmark for
 713 language-conditioned policy learning for long-horizon robot manipulation tasks. *IEEE Robotics*
 714 *and Automation Letters (RA-L)*, 7(3):7327–7334, 2022.

715

716 Chuan Min, Yongjun Pan, Wei Dai, Ibna Kawsar, Zhixiong Li, and Gengxiang Wang. Trajectory
 717 optimization of an electric vehicle with minimum energy consumption using inverse dynamics
 718 model and servo constraints. *Mechanism and Machine Theory*, 181:105185, 2023.

719

720 Abby O'Neill, Abdul Rehman, Abhinav Gupta, Abhiram Maddukuri, Abhishek Gupta, Ab-
 721 hishek Padalkar, Abraham Lee, Acorn Pooley, Agrim Gupta, Ajay Mandlekar, et al. Open x-
 722 embodiment: Robotic learning datasets and rt-x models. *arXiv preprint arXiv:2310.08864*, 2023.

723

724 Karl Pertsch, Kyle Stachowicz, Brian Ichter, Danny Driess, Suraj Nair, Quan Vuong, Oier Mees,
 725 Chelsea Finn, and Sergey Levine. Fast: Efficient action tokenization for vision-language-action
 726 models. *arXiv preprint arXiv:2501.09747*, 2025.

727

728 Alexander Pritzel, Benigno Uria, Sriram Srinivasan, Adria Puigdomenech Badia, Oriol Vinyals,
 729 Demis Hassabis, Daan Wierstra, and Charles Blundell. Neural episodic control. In *International*
 730 *conference on machine learning*, pp. 2827–2836. PMLR, 2017.

731

732 Alec Radford, Jong Wook Kim, Chris Hallacy, Aditya Ramesh, Gabriel Goh, Sandhini Agarwal,
 733 Girish Sastry, Amanda Askell, Pamela Mishkin, Jack Clark, et al. Learning transferable visual
 734 models from natural language supervision. In *International conference on machine learning*, pp.
 735 8748–8763. PMLR, 2021.

736

737 Ilija Radosavovic, Tete Xiao, Stephen James, Pieter Abbeel, Jitendra Malik, and Trevor Darrell.
 738 Real-world robot learning with masked visual pre-training. In *Conference on Robot Learning*, pp.
 739 416–426. PMLR, 2023.

740

741 Moritz Reuss, Ömer Erdinç Yağmurlu, Fabian Wenzel, and Rudolf Lioutikov. Multimodal dif-
 742 fusion transformer: Learning versatile behavior from multimodal goals, 2024. URL <https://arxiv.org/abs/2407.05996>.

743

744 Lucy Xiaoyang Shi, Brian Ichter, Michael Equi, Liyiming Ke, Karl Pertsch, Quan Vuong, James
 745 Tanner, Anna Walling, Haohuan Wang, Niccolo Fusai, et al. Hi robot: Open-ended instruction
 746 following with hierarchical vision-language-action models. *arXiv preprint arXiv:2502.19417*,
 747 2025.

748

749 Yang Tian, Sizhe Yang, Jia Zeng, Ping Wang, Dahua Lin, Hao Dong, and Jiangmiao Pang. Pre-
 750 dictive inverse dynamics models are scalable learners for robotic manipulation. *arXiv preprint*
 751 *arXiv:2412.15109*, 2024.

752

753 Endel Tulving. Episodic memory: From mind to brain. *Annual review of psychology*, 53(1):1–25,
 754 2002.

755

756 Endel Tulving et al. Episodic and semantic memory. *Organization of memory*, 1(381-403):1, 1972.

757

758 Homer Walke, Kevin Black, Abraham Lee, Moo Jin Kim, Max Du, Chongyi Zheng, Tony Zhao,
 759 Philippe Hansen-Estruch, Quan Vuong, Andre He, Vivek Myers, Kuan Fang, Chelsea Finn, and
 760 Sergey Levine. Bridgedata v2: A dataset for robot learning at scale, 2023.

756 Youpeng Wen, Junfan Lin, Yi Zhu, Jianhua Han, Hang Xu, Shen Zhao, and Xiaodan Liang. Vid-
 757 man: Exploiting implicit dynamics from video diffusion model for effective robot manipulation.
 758 *Advances in Neural Information Processing Systems*, 37:41051–41075, 2024.

759

760 Hongtao Wu, Ya Jing, Chilam Cheang, Guangzeng Chen, Jiafeng Xu, Xinghang Li, Minghuan Liu,
 761 Hang Li, and Tao Kong. Unleashing large-scale video generative pre-training for visual robot
 762 manipulation. *arXiv preprint arXiv:2312.13139*, 2023.

763

764 Weilai Xiang, Hongyu Yang, Di Huang, and Yunhong Wang. Denoising diffusion autoencoders are
 765 unified self-supervised learners. In *Proceedings of the IEEE/CVF International Conference on
 766 Computer Vision*, pp. 15802–15812, 2023.

767

768 Zhuoyi Yang, Jiayan Teng, Wendi Zheng, Ming Ding, Shiyu Huang, Jiazheng Xu, Yuanming Yang,
 769 Wenyi Hong, Xiaohan Zhang, Guanyu Feng, et al. Cogvideox: Text-to-video diffusion models
 770 with an expert transformer. *arXiv preprint arXiv:2408.06072*, 2024.

771

772 Seonghyeon Ye, Joel Jang, Byeongguk Jeon, Sejune Joo, Jianwei Yang, Baolin Peng, Ajay Man-
 773 dlekar, Reuben Tan, Yu-Wei Chao, Bill Yuchen Lin, et al. Latent action pretraining from videos.
 774 *arXiv preprint arXiv:2410.11758*, 2024.

775

776 Tianhe Yu, Deirdre Quillen, Zhanpeng He, Ryan Julian, Karol Hausman, Chelsea Finn, and Sergey
 777 Levine. Meta-world: A benchmark and evaluation for multi-task and meta reinforcement learning.
 778 In *Conference on robot learning*, pp. 1094–1100. PMLR, 2020.

779

780 Renrui Zhang, Jiaming Han, Chris Liu, Peng Gao, Aojun Zhou, Xiangfei Hu, Shilin Yan, Pan Lu,
 781 Hongsheng Li, and Yu Qiao. Llama-adapter: Efficient fine-tuning of language models with zero-
 782 init attention. *arXiv preprint arXiv:2303.16199*, 2023.

783

784 Renrui Zhang, Dongzhi Jiang, Yichi Zhang, Haokun Lin, Ziyu Guo, Pengshuo Qiu, Aojun Zhou,
 785 Pan Lu, Kai-Wei Chang, Peng Gao, et al. Mathverse: Does your multi-modal llm truly see the
 786 diagrams in visual math problems? *ECCV 2024*, 2024a.

787

788

789

790

791

792

793

794

795

796

797

798

799

800

801

802

803

804

805

806

807

808

809

810
811 **SUPPLEMENTAL MATERIAL**
812813 To better understanding of this work, we offer additional details, analysis, and results as follows:
814

- 815 • **A Use of Large Language Models, Ethics Statement, and Reproducibility Statement**
816 In this section, we clarify the use of LLMs, the ethics statement, and the reproducibility
817 statement in our paper, which primarily served as assistants for refining and polishing the
818 paper during the writing process.
819
- 820 • **B Implementation Details**
821 In this section, we present the implementation details of TriVLA and its inherent Episodic
822 World Model, including the training procedure and rollout process.
823
- 824 • **C Demo Video**
825 In this section, we present the performance of TriVLA on short-horizon and long-horizon
826 tasks to verify the practical effect of the Episodic World Model.
827
- 828 • **D Comparison Methods**
829 In this section, we select a representative subset of prior methods for comparison.
830
- 831 • **E Details and More Results of Episodic Dynamics Perception**
832 In this section, we present detailed visualizations and results for Episodic Dynamics Per-
833 ception in TriVLA. We employ a stable video diffusion model as the core module for
834 Episodic Dynamics Perception and visualize the intermediate predictive representations
835 through one-step and full step predictions.
836
- 837 • **F Qualitative Analysis and Results.**
838 This section presents comprehensive experiments on simulated and real-world tasks to eval-
839 uate the TriVLA framework. The simulated experiments employ three benchmarks that en-
840 compass diverse robot embodiments and manipulation tasks. In parallel, real-world trials
841 evaluate long-horizon tabletop manipulation using a Kinova Gen3 robotic arm.
842
- 843 • **G Real-world Experiments**
844 In this section, we present a series of real-world experiments designed to rigorously eval-
845 uate the practical applicability, task generalization, and operational robustness of our
846 TriVLA framework under realistic and unstructured environments.
847

848 **A USE OF LARGE LANGUAGE MODELS, ETHICS STATEMENT, AND**
849 **REPRODUCIBILITY STATEMENT**
850851 A.1 USE OF LARGE LANGUAGE MODELS (LLMs)
852853 In preparing this paper, we used ChatGPT-4o (OpenAI) as a general-purpose writing assistance
854 tool. Its role was strictly limited to checking and improving spelling, grammar, and sentence-level
855 clarity. The LLM did not contribute to the conception of the research idea, experimental design, data
856 analysis, interpretation of results, or the drafting of any substantive scientific content. All intellectual
857 contributions, arguments, and conclusions presented in this paper are our own.
858859 A.2 ETHICS STATEMENT
860861 TriVLA advances vision–language–action (VLA) research by introducing an episodic world model
862 that enables embodied agents to accumulate, recall, and predict sequential experiences for ro-
863 bust, long-horizon decision-making. This capability lowers barriers to building more generalizable
864 and intelligent robots, which can benefit applications in assistive robotics, manufacturing, and hu-
865 man–robot interaction. At the same time, these advances raise ethical considerations regarding po-
866 tential misuse (e.g., autonomous systems acting beyond intended safety boundaries, reinfor-
867 cements of social or cultural biases in pretrained vision–language models) and broader societal impacts (e.g.,
868 displacement of human labor or over-reliance on autonomous decision-making). We encourage fur-
869 ther research into transparent evaluation, safety alignment, and bias mitigation, as well as careful
870 consideration of the ethical implications when deploying such systems in real-world settings.
871

864 A.3 REPRODUCIBILITY STATEMENT
865866 We are committed to ensuring the reproducibility of all results reported in this work. Upon pub-
867 lication, we will release the TriVLA codebase, pretrained checkpoints for all system components
868 (vision-language model, video diffusion model, and policy network), as well as training and eval-
869 uation scripts. Detailed descriptions of the episodic world model architecture, triple-system inte-
870 gration, and flow-matching mechanisms are provided in Supplemental Material B, along with the
871 hyperparameters and dataset preprocessing steps. We also specify all benchmarks, metrics, and ex-
872 perimental protocols used in both simulated and real-world evaluations. To facilitate independent
873 verification, we will include environment setup instructions, hardware requirements, and example
874 configurations, ensuring the seamless replication of our results.
875876 B IMPLEMENTATION DETAILS
877878 B.1 TRAINING DETAILS.
879880 As detailed in Section 4, we employ a unified triple-system architecture. System 2, the Episodic
881 Multimodal Perception, utilizes the pretrained Eagle-2 VLM for processing visual and language
882 inputs on an NVIDIA H100 GPU. System 3 fine-tunes a video foundation model for manipulation-
883 centric Episodic Dynamics Perception using 193,690 human Goyal et al. (2017) and 179,074
884 robotic O’Neill et al. (2023) trajectories, supplemented by videos from CALVIN ABC, MetaWorld,
885 and real-world tasks. To mitigate dataset discrepancies, we adopt dataset-specific sampling ratios
886 following Octo. Video model fine-tuning requires 2–3 days on 8 NVIDIA H100 GPUs. The gener-
887 alist policy is subsequently trained on task datasets, taking 5–9 hours on four H100 GPUs.
888889 B.2 ROLL-OUT DETAILS.
890891 The System 2 Episodic Multimodal Perception module employs a pretrained Eagle-2 VLM to ex-
892 tract vision-language tokens, operating at 36.36 Hz on an NVIDIA H100 GPU. In contrast to prior
893 methods, which utilize computationally intensive video denoising—resulting in low control fre-
894 quencies Black et al. (2023) or open-loop limitations Du et al. (2024)—our approach processes each
895 observation through System 2 only once, during the initial forward pass of the Episodic Dynamics
896 Perception module, with inference latency below 85.9 ms. Subsequently, the downstream policy
897 generates a 10-step action chunk Chi et al. (2023), enabling control frequencies of 34–36 Hz on a
898 consumer-grade NVIDIA RTX H100 GPU.
899900 C DEMO VIDEO
901902 The attached video demonstrates the application of TriVLA, a triple-system architecture inspired by
903 cognitive neuroscience, designed to enhance the capabilities of embodied agents in complex tasks.
904 TriVLA integrates an episodic world model, enabling robots to accumulate, recall, and predict se-
905 quential multimodal experiences. This model provides the foundation for robust, adaptive control
906 by simulating episodic memory processes. This showcases the generalization ability of the TriVLA
907 framework. The tasks in the video highlight how TriVLA’s high-level reasoning and dynamic predic-
908 tion enable robots to handle long-horizon manipulation and understand complex prompts, demon-
909 strating its capability for sophisticated, adaptable decision-making.
910911 The following is a detailed explanation of the tasks that TriVLA handles in the video.
912913 C.1 VISUALIZATION OF EPISODIC DYNAMICS PERCEPTION
914915 This demo presents the Episodic Dynamics Perception capability of TriVLA in real-world scenarios.
916 By utilizing a stable video diffusion model, TriVLA encodes the current scene and anticipates future
917 dynamics over long time horizons. The visualization highlights ground-truth outcomes, single-step
918 predictions, and full-sequence forecasts, demonstrating how the model captures essential motion
919 cues such as object interactions and robotic arm trajectories. These results show that TriVLA can
920 effectively model entire video sequences and predict future states based on current observations and
921

918 task instructions, enabling a deeper understanding of physical dynamics for downstream decision-
 919 making and action planning.
 920

921 C.2 VISUALIZATION OF ACTION TRAJECTORY IN SIMULATION 922

923 This demo illustrates the action trajectory generation of TriVLA in a simulated environment. We
 924 showcase three representative examples of action sequences executed under multiple consecutive
 925 instructions, such as “Pull the handle to open the drawer,” “Grasp and lift the pink block,” “Use
 926 the switch to turn on the light bulb,” and “Store the grasped block in the sliding cabin.” TriVLA
 927 demonstrates its ability to comprehend complex instructions, infer underlying intent, and leverage
 928 predictive modeling to plan and execute long-horizon tasks. By combining high-level reasoning
 929 from vision-language models (VLMs) with dynamic predictive representations from video diffusion
 930 models (VDMs), TriVLA integrates world knowledge to enhance intent understanding and predicts
 931 future states to guide sequential decision-making. These results highlight how TriVLA effectively
 932 coordinates perception, reasoning, and prediction to accomplish complex, multi-step tasks in simu-
 933 lation.
 934

935 C.3 VISUALIZATION OF ACTION TRAJECTORY IN SHORT-HORIZON REAL-WORLD TASKS 936

937 Across the four short-horizon tasks—folding a pink towel, grasping an orange and placing it on a
 938 purple plate, pouring water from a green cup into a purple cup, and relocating a cup to the right
 939 side—the TriVLA consistently demonstrates its capability for precise, reliable, and context-aware
 940 manipulation. These tasks collectively highlight the model’s versatility: from handling deformable
 941 objects to executing accurate pick-and-place operations and controlling dynamic pouring actions. By
 942 integrating real-time visual perception with adaptive motor planning, TriVLA achieves robust short-
 943 horizon performance, ensuring accurate execution under diverse manipulation challenges. This suite
 944 of tasks underscores TriVLA’s efficiency in short-term control, where rapid perception-action cou-
 945 pling is critical for success.

946 **Short-horizon Task: “Fold Towel”** In this scenario, the TriVLA demonstrates its capacity to ma-
 947 nipulate deformable objects by folding a pink towel with precision. This task requires careful han-
 948 dling of soft materials, demanding spatial reasoning beyond rigid object grasping. The policy lever-
 949 ages its perception to recognize the towel’s shape and orientation, planning an appropriate folding
 950 trajectory. Through this task, TriVLA highlights its short-horizon ability to interact with deformable
 951 objects in a controlled manner.

- 952 • TriVLA achieves this by adjusting its grasp and fold strategy in real-time, ensuring the
 953 towel is folded along the intended line.
- 954 • The success of this task emphasizes TriVLA’s adaptability in dealing with non-rigid ob-
 955 jects, integrating visual cues into consistent action sequences.

956 **Short-horizon Task: “Grasp Orange”** In this scenario, the TriVLA showcases its skill in precise
 957 object manipulation by picking up an orange and placing it onto a purple plate. The task requires
 958 accurate localization and trajectory control, as the system must not only grasp the fruit securely but
 959 also transport it safely to the designated location. Through this task, TriVLA demonstrates its ability
 960 to carry out reliable short-horizon pick-and-place operations.

- 962 • TriVLA accomplishes this by dynamically refining its grasp and movement trajectory based
 963 on real-time feedback.
- 964 • The successful completion highlights TriVLA’s integration of perception and motion plan-
 965 ning, enabling robust execution of targeted placement tasks.

967 **Short-horizon Task: “Pouring”** In this scenario, the TriVLA demonstrates its ability to perform
 968 liquid transfer by grasping a green cup and pouring water into a purple cup. This task requires
 969 stable control of orientation and precise alignment between the two containers, ensuring minimal
 970 spillage. The policy leverages its multimodal perception to model both rigid object states and the
 971 flow dynamics of the liquid. Through this task, TriVLA demonstrates competence in controlled
 972 pouring, a challenging short-horizon manipulation.

972

- 973 • TriVLA achieves this by continuously monitoring the cup angle and relative position to
- 974 regulate water flow.
- 975 • The success of this task highlights TriVLA’s ability to coordinate fine-grained motor control
- 976 with visual guidance for dynamic object interaction.

977 **Short-horizon Task: “Pick Cup”** In this scenario, the TriVLA performs a straightforward relo-
 978 cation task by picking up a cup from the table and placing it on the right side. While simple, this
 979 task demands accurate detection of the cup’s position and a reliable transfer motion without dis-
 980 rupting the environment. Through this task, TriVLA showcases its efficiency in executing basic,
 981 short-horizon manipulation.

982

- 983 • TriVLA achieves this by generating a direct grasp-to-place trajectory, adapting its motion
- 984 based on sensory feedback.
- 985 • The success of this task demonstrates TriVLA’s ability to reliably execute fundamental
- 986 pick-and-place operations with consistency.

988 **C.4 VISUALIZATION OF ACTION TRAJECTORY IN LONG-HORIZON REAL-WORLD TASKS**

990 **Long-horizon Task: “Beverage Preparation”** In this scenario, the TriVLA demonstrates its com-
 991 petence in executing a complex, sequential task: picking up a red beverage can from the shelf,
 992 pouring the beverage into a yellow cup, inserting a straw into the yellow cup, and finally pushing
 993 the cup forward. Unlike short-horizon manipulations, this task requires the integration of multiple
 994 atomic actions into a coherent sequence, demanding sustained spatial reasoning, memory of inter-
 995 mediate states, and precise coordination across distinct phases. Through this task, TriVLA show-
 996 cases its ability to plan and execute long-horizon activities where success depends on maintaining
 997 consistency across multiple dependent steps.

998

- 999 • TriVLA achieves this by decomposing the task into sub-goals, dynamically adjusting its
- 1000 strategy based on real-time perception and the evolving state of the environment.
- 1001 • The successful completion highlights TriVLA’s ability to combine high-level planning with
- 1002 fine-grained control, ensuring the transition is seamless and reliable.
- 1003 • This task demonstrates TriVLA’s strength in long-horizon reasoning, where sustained ac-
 1004 tion sequences and contextual understanding are essential for achieving complex goals.

1005 TriVLA’s episodic world model enables robots to simulate memory processes, allowing them to
 1006 accumulate sequential experiences and predict future actions. This capability helps robots adapt dy-
 1007 namically to changing environments and illustrates how embodied agents can reason about actions
 1008 and experiences in a human-like way. It adopts a triple-system architecture that integrates episodic
 1009 memory, high-level reasoning, and dynamic prediction. This unified design allows robots to under-
 1010 stand multi-step tasks, solve complex manipulation problems, and make decisions grounded in both
 1011 past experiences and anticipated outcomes.

1012 In summary, TriVLA provides a robust framework for robots, offering spatial-temporal awareness,
 1013 high-level reasoning, and adaptive control over long horizons. The model demonstrates exceptional
 1014 generalization ability, enabling robots to perform tasks in diverse, complex environments.

1016 **D COMPARISON METHODS**

1019 Generalist robot policies have been extensively investigated in prior research. In our experiments, we
 1020 select a representative subset of prior methods for comparison, focusing on those that have achieved
 1021 state-of-the-art performance or employ approaches similar to ours.

1022

- 1023 • RT-1 Brohan et al. (2022): A general action learning robot policy integrating semantic
- 1024 features via Efficient-Net with FiLM-conditioning, subsequently employing token learners.
- 1025 • Diffusion Policy Chi et al. (2023): A action learning approach modeling the robot’s visuo-
 1026 motor policy as a conditional denoising diffusion process enhanced with action diffusers.

- Robo-Flamingo Li et al. (2023b): A direct action learning policy leveraging a pre-trained LLM, integrating visual information into each layer following the Flamingo Alayrac et al. (2022).
- UniPi Du et al. (2024): Initiates by training a video prediction model for future sequence generation and concurrently learns an inverse kinematics model between frames to infer actions.
- MDT Reuss et al. (2024): Trains a diffusion transformer-based policy complemented by an auxiliary MAE loss to facilitate future state reconstruction.
- Susie Black et al. (2023): Employs a fine-tuned InstructPix2Pix Brooks et al. (2023) model to generate goal images and trains a downstream diffusion policy conditioned on these goal images.
- GR-1 Wu et al. (2023): Models video and action sequences using an autoregressive transformer. During policy execution, GR-1 predicts one future frame followed by a action.
- Robo-Uniview Liu et al. (2024b): Develops a 3D-aware visual encoder supervised by a 3D occupancy loss for policy learning.
- Vidman Wen et al. (2024): Pre-trained on the Open X-Embodiment video dataset, it employs a self-attention adapter to convert video representations into policies. However, Vidman’s performance is suboptimal due to the absence of fine-tuning the video model on downstream tasks.
- Seer Tian et al. (2024): Designs a novel end-to-end framework that leverages predictive inverse dynamics models to integrate vision and action for scalable robotic manipulation.
- VPP Hu et al. (2024): Leverages video diffusion models to generate visual representations, addressing the limitations of traditional vision encoders in capturing temporal aspects critical for robotic manipulation.

E DETAILS AND MORE RESULTS OF EPISODIC DYNAMICS PERCEPTION

We employ a stable video diffusion model as the dynamics perception module, performing a single forward pass to obtain visual representations that encompass both current static information and predicted future dynamics. As illustrated in Figure 7, we present visualizations of ground-truth futures alongside single-step and full-step predictions on the Bridge benchmark. The visualization results indicate that single-step representations convey critical information, including object and robot arm motion, thereby effectively supporting downstream action learning. The dynamics perception module models entire video sequences and predicts future frames conditioned on current observations and instructions, demonstrating a sound understanding of physical dynamics.

Additionally, we extend our analysis to real-world experiments, where we replicate the same predictive framework on an actual robot. As shown in Figure 8 and 9, the true-to-life experimental results mirror the findings from the simulated setup, further validating the robustness of our prediction model. These real-world predictions are crucial, as they show that our system not only captures the motion of objects and the robot arm but also adapts to real-world uncertainties, such as sensor noise and minor mechanical inaccuracies.

The real-world prediction visualizations highlight several important aspects of our approach:

- Accurate Motion Forecasting: Even in the face of real-world complexities, the system accurately predicts future motions of both the robot arm and surrounding objects. This is key for enabling high-level decision-making and adaptive action execution.
- Real-World Generalization: The model demonstrates strong generalization capabilities, transferring learned predictions from the benchmark environment to practical settings without requiring extensive retraining. The system’s robustness in handling real-world dynamics proves the versatility of the proposed architecture.

By leveraging these visualizations and predictions in both the simulated and real environments, we show that our framework can bridge the gap between theoretical modeling and real-world robotic applications. This provides a powerful tool for task generalization, enabling robots to efficiently

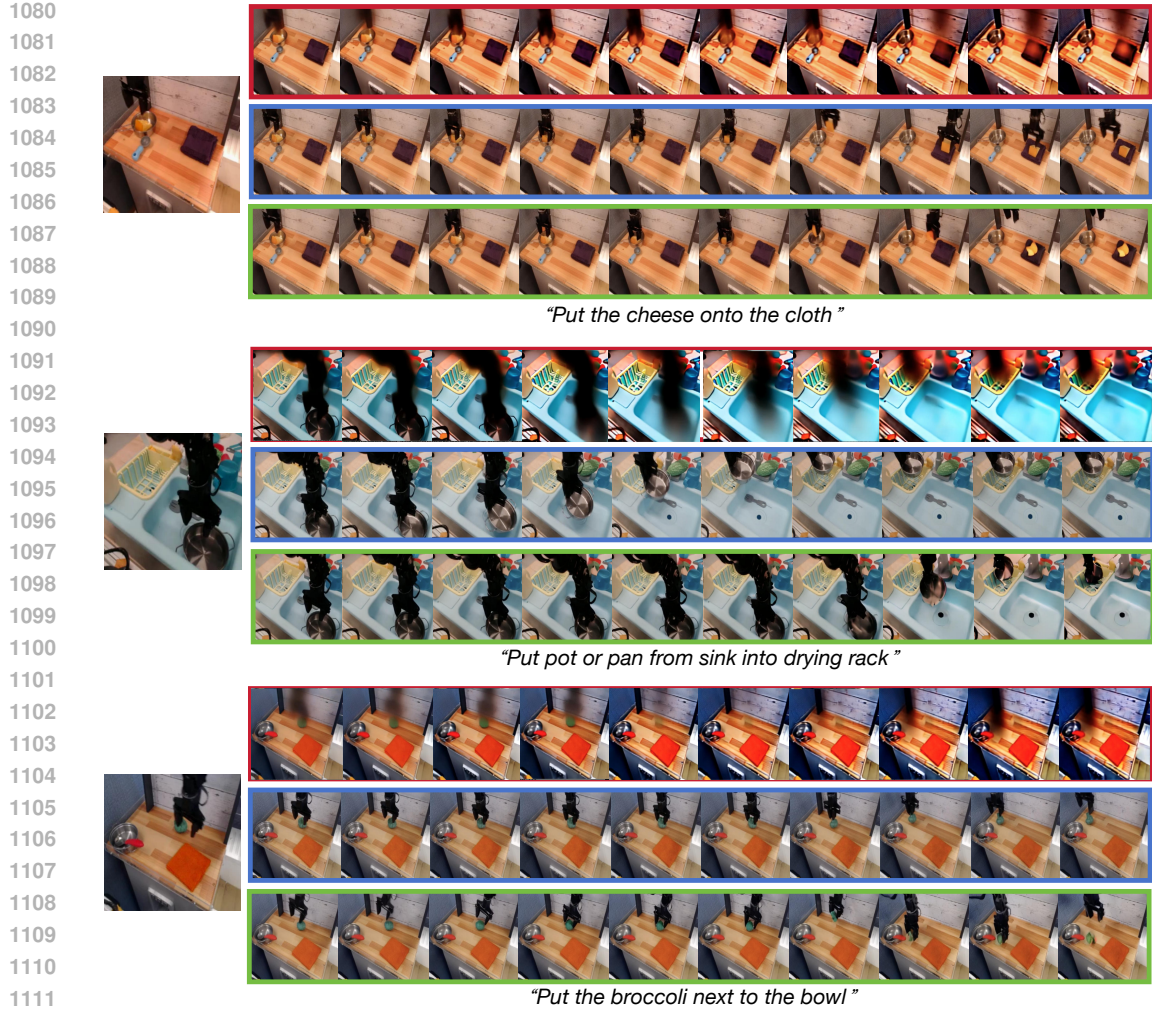


Figure 7: **Visualization of Episodic Dynamics Perception on the Bridge Benchmark.** The red box indicates one-step prediction, the blue box corresponds to full-step prediction, and the green box marks the ground truth. We can observe that the representation can provide valuable information on physical dynamics, although the textures and details are not precise enough.

plan and execute complex actions in diverse scenarios. In summary, the combination of simulated and real-world results not only validates the robustness of our prediction framework but also underscores its potential for real-time action learning and autonomous decision-making in physical environments. The visualizations of future predictions further support the importance of incorporating dynamic modeling into robotic systems, fostering a deeper understanding of physical interactions and improving the overall system performance.

F QUALITATIVE ANALYSIS AND RESULTS

We provide qualitative examples of action sequences generated by TriVLA in Figure 10. Given multiple consecutive instructions—for instance, “Pull the handle to open the drawer,” “Grasp and lift the pink block,” “Use the switch to turn on the light bulb,” and “Store the grasped block in the sliding cabin”—TriVLA demonstrates the ability to comprehend instructions, infer intent, and utilize predictive capabilities to accomplish long-horizon tasks. The results demonstrate that TriVLA employs VLMs and VDMs for both high-level reasoning based on common knowledge and dynamic predictive representation provided by a world model. TriVLA integrates world knowledge to enhance intent understanding and utilizes a world model for future state prediction when processing multiple sequential instructions, thereby enabling effective long horizon task execution.

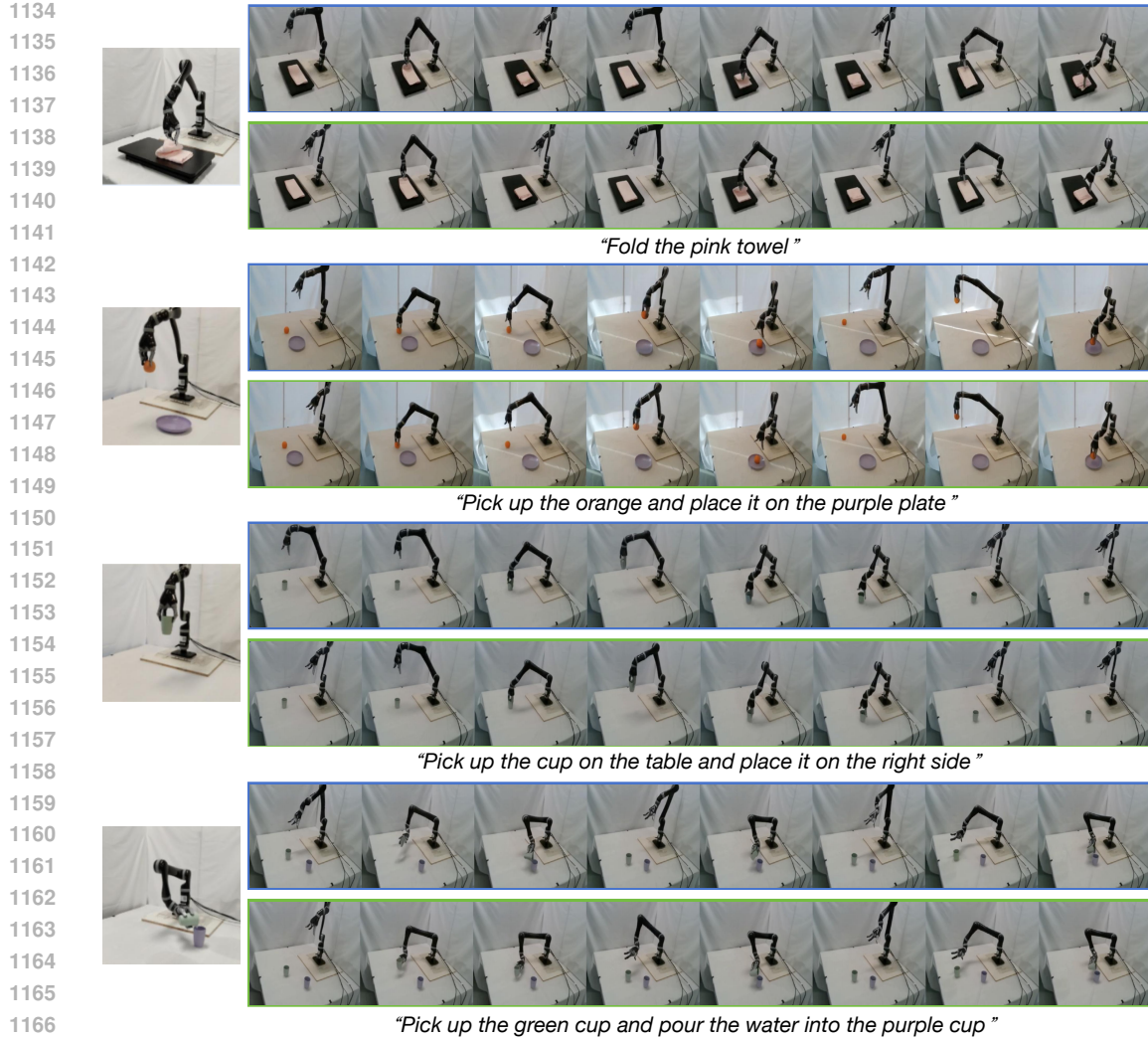


Figure 8: **Visualization of Episodic Dynamics Perception on Real-world Tasks.** The blue box corresponds to the full-step prediction, and the green box marks the ground truth of the current timestep. We can observe that representation can provide valuable information on physical dynamics, although the textures and details are not precise enough.

- Precise Alignment with Modeled Dynamics: Since simulation provides deterministic or near-deterministic dynamics, TriVLA demonstrates highly consistent outcomes across repeated trials. For instance, during multi-step manipulation sequences, object trajectories match predicted states almost perfectly, showcasing the model’s capability to exploit stable environments for accurate planning.
- Stress Testing under Controlled Perturbations: Simulation allows for the systematic injection of domain variations, such as randomized object masses, altered friction coefficients, or unexpected collisions. TriVLA adapts to these controlled perturbations by updating its predictions accordingly, highlighting its resilience under a wide spectrum of simulated uncertainties.
- Long-Horizon Reasoning at Scale: Most importantly, simulation provides an ideal platform for TriVLA to validate long-horizon planning strategies across diverse scenarios. By anticipating future states over extended horizons, the model learns to optimize its policy in a wide variety of contexts, generating transferable skills that can later be fine-tuned for real-world execution.

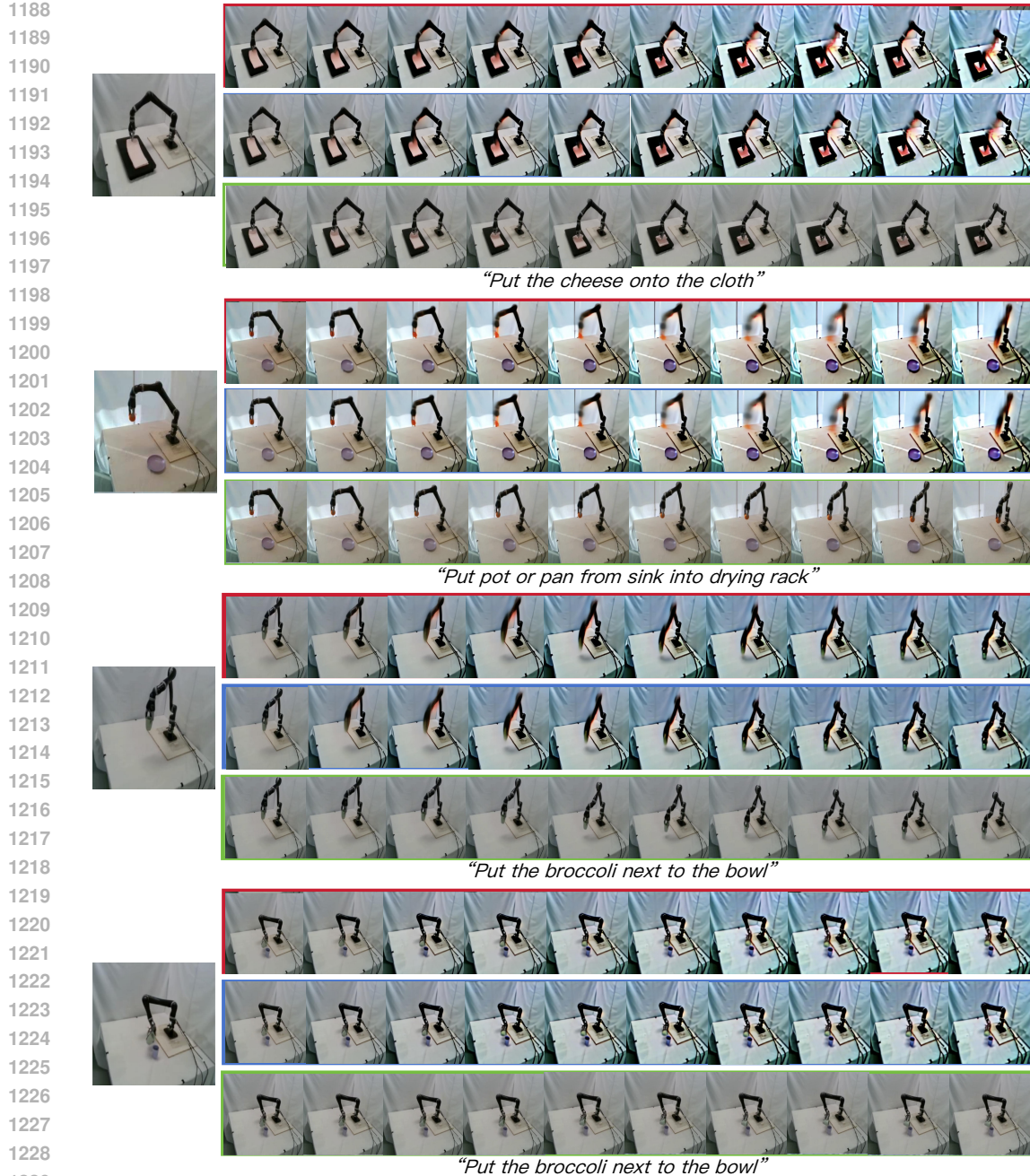


Figure 9: **Visualization of Episodic Dynamics Perception on Real-world Tasks.** The red box indicates the one-step prediction, the blue box corresponds to the full-step prediction, and the green box marks the ground truth. We can observe that representation can provide valuable information on physical dynamics, although the textures and details are not precise enough.

G REAL-WORLD EXPERIMENTS

In addition to the simulated results, we also conducted real-world experiments, where TriVLA successfully generates and executes action sequences on a physical robot. As shown in Figure 11, the robot accurately follows the same sequence of tasks, starting from pulling the handle to opening the drawer, grasping and lifting the pink block, using the switch to turn on the light bulb, and finally storing the block in the sliding cabin. These real-world results closely align with the predictions

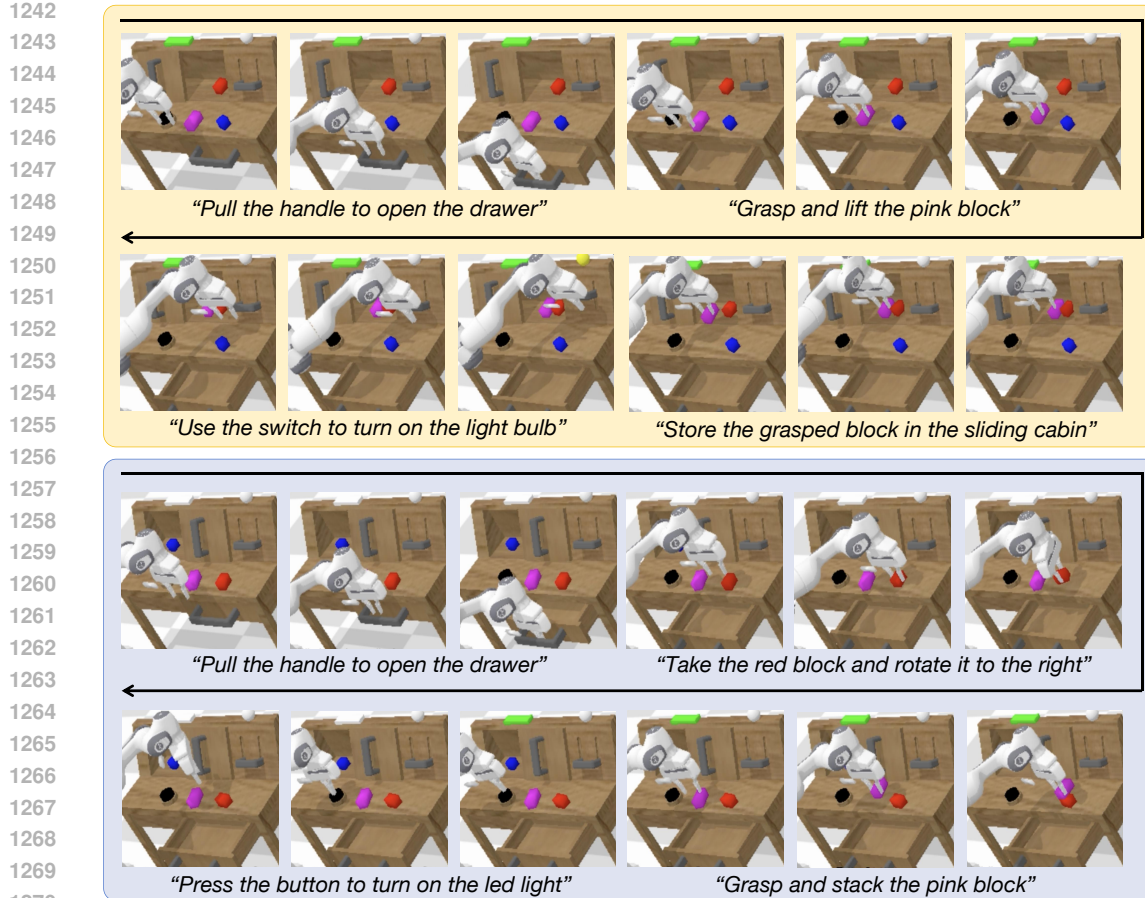


Figure 10: **Qualitative case study of CALVIN benchmark.** Our TriVLA performs strongly in long-horizon missions. For example, in the CALVIN simulation task, it integrates world knowledge to interpret intent and uses a world model to predict future states. Given multiple sequential instructions, TriVLA can effectively execute long-horizon tasks.

and actions generated in the simulated environment, further validating TriVLA’s ability to handle complex, multi-step tasks in dynamic, real-world scenarios.

The real-world experiments highlight several key advantages of TriVLA’s approach:

- **Real-Time Sequence Execution:** The robot efficiently processes and executes long-horizon tasks in real-time, leveraging TriVLA’s ability to predict intermediate states and adjust actions accordingly. Despite the inherent variability and unpredictability of the real world, such as slight environmental changes or sensor noise, TriVLA’s predictive capabilities allow the robot to remain on task without requiring extensive retraining.
- **High Fidelity in Task Completion:** As the robot progresses through the sequence of actions, it demonstrates a strong alignment between predicted outcomes and actual results. For instance, after pulling the handle, the drawer opens correctly, and the robot adjusts its grip on the block while maintaining stability during the lift. This showcases the robustness of TriVLA’s predictive world model in real-world settings.
- **Dynamic Adaptation to Uncertainty:** The real-world setup also presents challenges like minor inaccuracies in motor control or shifting environmental conditions. TriVLA exhibits impressive adaptability, dynamically adjusting predictions and actions to account for these uncertainties, ensuring continued task success.
- **Long-Horizon Task Planning:** Perhaps most notably, TriVLA demonstrates its ability to execute long-horizon plans by integrating both episodic memory and predictive reasoning. By leveraging its world model, TriVLA is able to anticipate future states and proactively



1322 **Figure 11: Qualitative case study of real-world tasks.** Our **TriVLA** performs well in real-world
 1323 tasks, successfully executing both short-horizon and long-horizon manipulations. The results illus-
 1324 trate its ability to integrate perception, prediction, and control for reliable task completion under
 1325 real-world conditions.

1326
 1327 adjust actions, ensuring that all steps of the sequence are successfully completed, even in
 1328 the presence of unforeseen challenges.

1329
 1330 Overall, these real-world experiments reinforce the core strength of **TriVLA**: its ability to understand
 1331 complex instructions, reason about sequential actions, and predict future states—an essential capa-
 1332 bility for enabling embodied agents to perform sophisticated tasks autonomously and effectively in
 1333 the real world. Through the combination of simulated and real-world action sequence generation,
 1334 **TriVLA** proves to be a highly capable architecture for long-horizon task execution, paving the way
 1335 for more advanced and adaptable autonomous systems.